

## Supplementary Materials for The generational scalability of single-cell replicative aging

Ping Liu and Murat Acar

Published 31 January 2018, *Sci. Adv.* **4**, eaao4666 (2018)

DOI: 10.1126/sciadv.aao4666

### This PDF file includes:

- fig. S1. Evaluating the Kolmogorov-Smirnov test on differentially scaled survival curves using simulated data.
- fig. S2. Parameter sweeps.
- fig. S3. Fit performance comparisons between one- and two-parameter Weibull survival functions.
- fig. S4. Predictive capacity characterization for the one-parameter Weibull survival function on 200 wild-type cells.
- fig. S5. Predictive capacity characterization for the one-parameter Weibull survival function on 1000 wild-type cells.
- fig. S6. Predictive capacity characterization for the one-parameter Weibull survival function on *sir2* $\Delta$ .
- fig. S7. Predictive capacity characterization for the one-parameter Weibull survival function on *rif1* $\Delta$ .
- fig. S8. Predictive capacity characterization for the one-parameter Weibull survival function on *tpi15* $\Delta$ .
- fig. S9. Predictive capacity characterization for the one-parameter Weibull survival function on *gpa2* $\Delta$ .
- fig. S10. Predictive capacity characterization for the one-parameter Weibull survival function on *tor1* $\Delta$ .
- fig. S11. Predictive capacity characterization for the one-parameter Weibull survival function on *fab1* $\Delta$ .
- fig. S12. Predictive capacity characterization for the one-parameter Weibull survival function on *sgf73* $\Delta$ .
- fig. S13. Quantifying deviations from perfect scaling.
- fig. S14. Simulation results for the Strehler-Mildvan model with vitality drift diffusion.

- fig. S15. Performance of the exponential challenge arrival process.
- fig. S16. Results from the application of AIC and BIC tests on the stochastic models tested.
- fig. S17. Sensitivity characterization for the Strehler-Mildvan model parameters.
- fig. S18. The generation-dependent dynamics of the aging or viability state  $X$ .
- fig. S19. Numerical connection between the Strehler-Mildvan and Weibull survival functions.
- table S1. Results from the Kolmogorov-Smirnov statistic  $\sup|S_i - S_j|$ , where  $\sup$  is the supremum (maximum) function.
- table S2.  $P$  values computed using `ks.test` function of R.
- table S3. Fit results from the use of the two-parameter Gompertz, gamma, and Weibull survival functions.
- table S4. Fit performance of the two-parameter Weibull survival function.
- table S5. Fit performance of the one-parameter Weibull survival function ( $\alpha$  is fixed at 3.28).
- table S6. Fit and prediction results from the use of the one-parameter Weibull survival function.
- table S7. Fit and prediction results from the use of the one-parameter Weibull survival function.
- table S8. Yeast strains used in this study.
- table S9. For each microscopic process, parameter ranges used during the sampling process and the fitted parameter values.
- table S10. Predicted parameter values for *sir2* $\Delta$  and *fab1* $\Delta$  strains, obtained after applying scaling.
- Supplementary Materials and Methods
- References (18, 19)

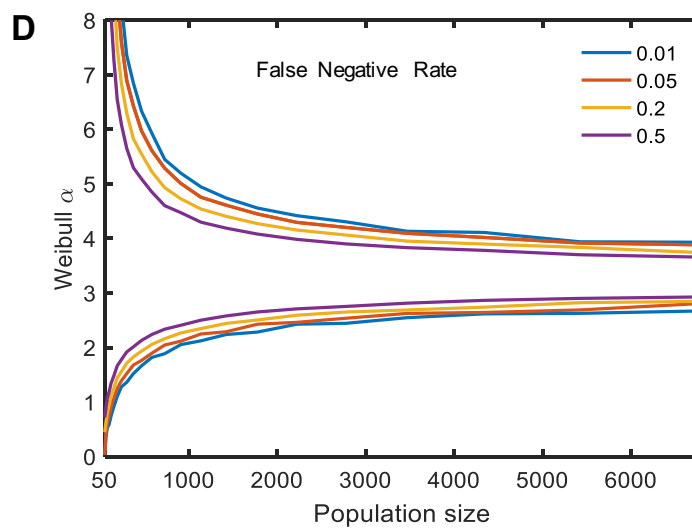
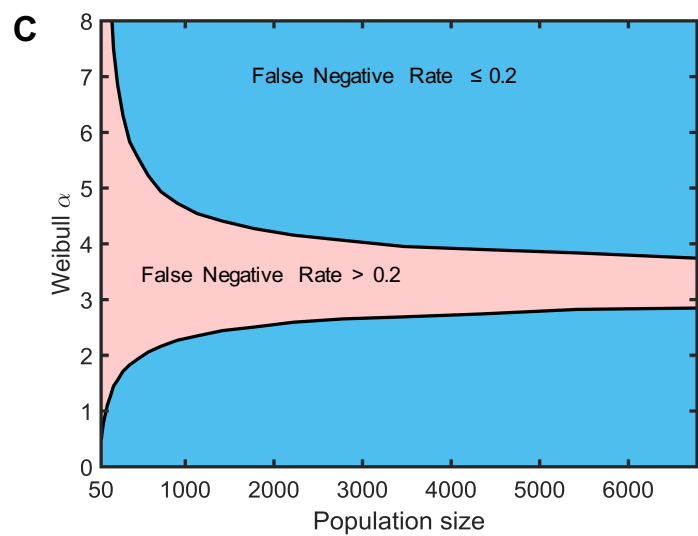
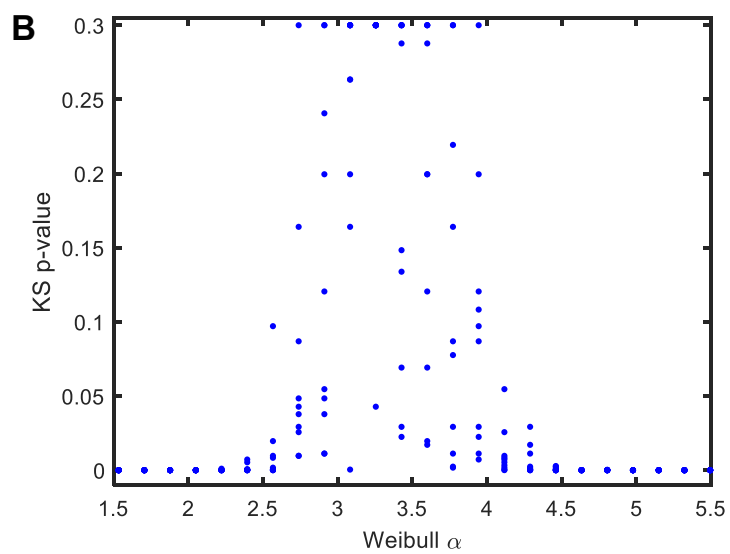
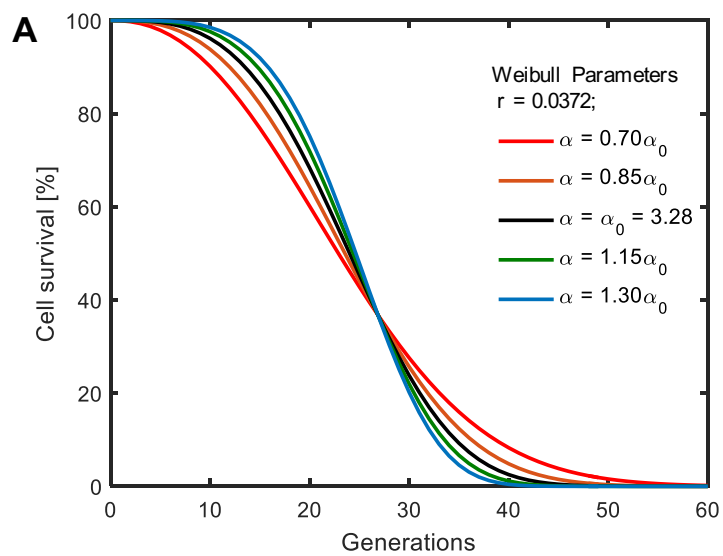


**Figure S1**

**fig. S1. Evaluating the Kolmogorov-Smirnov test on differentially scaled survival curves using simulated data.** **A.** By keeping the scaling parameter  $r$  at 0.0372 corresponding to the wild-type distribution (table S3), five sample survival curves (representing sample outcomes obtained after applying the AFT model) are shown. The curves were obtained by running the Weibull survival function at five different  $\alpha$  values around the value corresponding to the wild-type distribution (table S3). Changes in  $\alpha$  cause the simulated populations to deviate from the baseline population corresponding to the population obtained by using the best-fitting Weibull parameters for the wild-type population (table S3). **B.** Distribution of KS  $p$ -values across 24 different  $\alpha$  values swept between 1.5 and 5.5. The Weibull  $r$  parameter was fixed at 0.0372. Sets of death times containing 1500 samples were drawn from a Weibull distribution. Each population was compared to the baseline across replicate trials with a calculation of the KS  $p$ -value to estimate the likelihood that observed differences occurred by chance. All  $p$ -values larger than 0.3 were cropped at 0.3. **C.** Power of the KS-test with simulated data for population sizes varying between 50 and 6776 cells. The Weibull  $r$  is set at 0.0372. The plot indicates the minimum population size required to detect a given effect size (a difference in the Weibull  $\alpha$  to the reference population) at a statistical power of 0.8 (a false-negative rate of 0.2) and significance level (false-positive rate) of 0.0018. This number ( $0.0018 = 0.05/28$ ) corresponds to the significance level of 0.05 for the family of 28 pairwise comparisons between the 8 strains using Bonferroni's correction method for multiple hypothesis testing. The pink (blue) area indicates effect and population size combinations that yield a false-negative rate greater (less) than 0.2. **D.** Same as in panel (C), but for false-negative rates of 0.5, 0.2, 0.05, or 0.01.

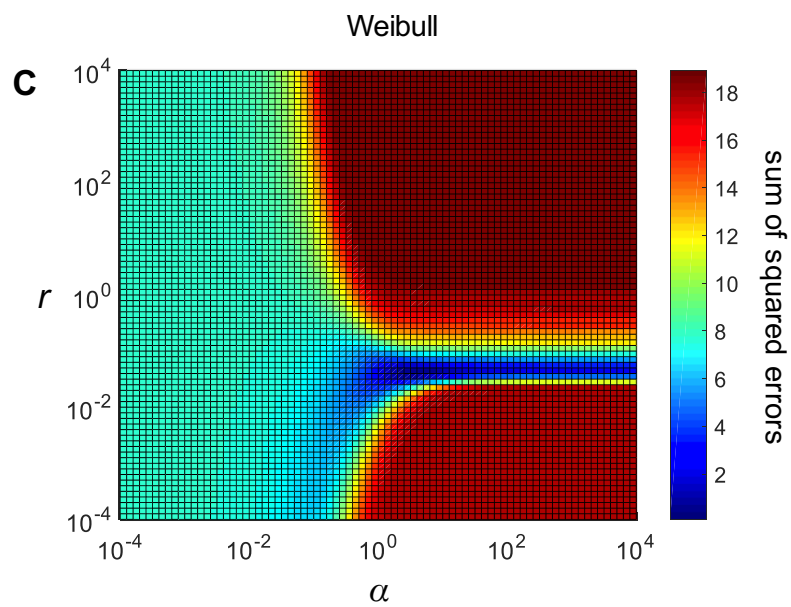
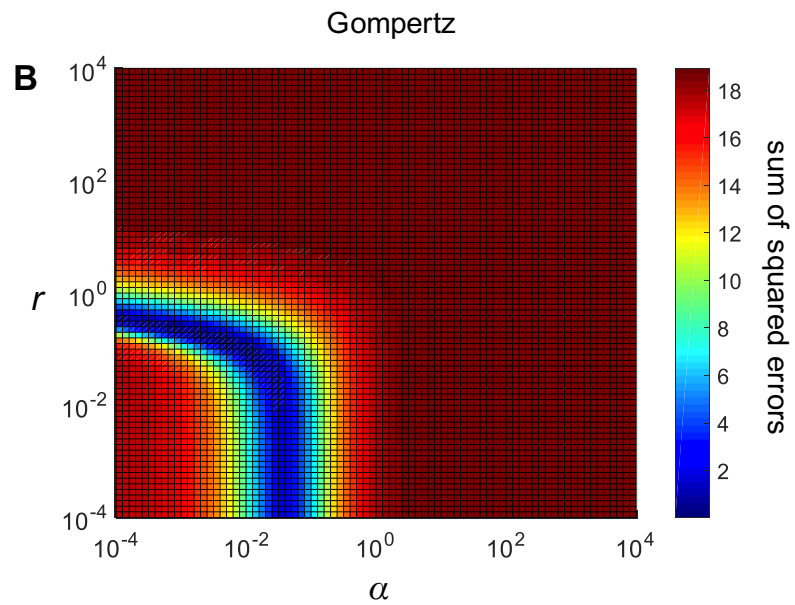
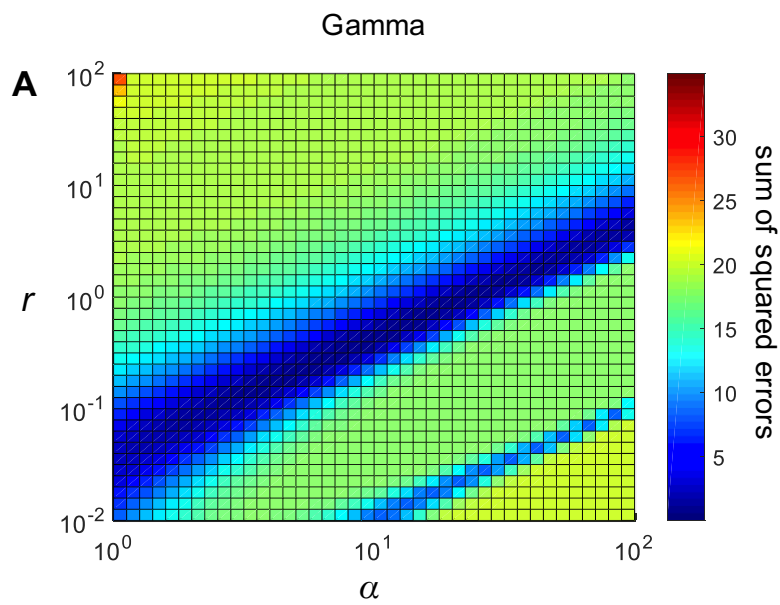


Figure S2

**fig. S2. Parameter sweeps. A-C.** Parameter values were systematically sampled from large ranges and sum of squared errors (SSE) were examined. SSEs were calculated by summing the squared differences (along the survival curve) between each experimental  $S/S_0$  value and the theoretical one obtained from each two-parameter function (gamma (**A**), Gompertz (**B**), Weibull (**C**)) when a pair of parameter values were fed to it. One global minimum value was seen in each plot (dense blue region) and each of the three fits shown in figure S2 converged to their respective minimum value displayed in **A-C** here.  $N=200$  wild type cells formed the experimental survival curve used in the SSE calculations.

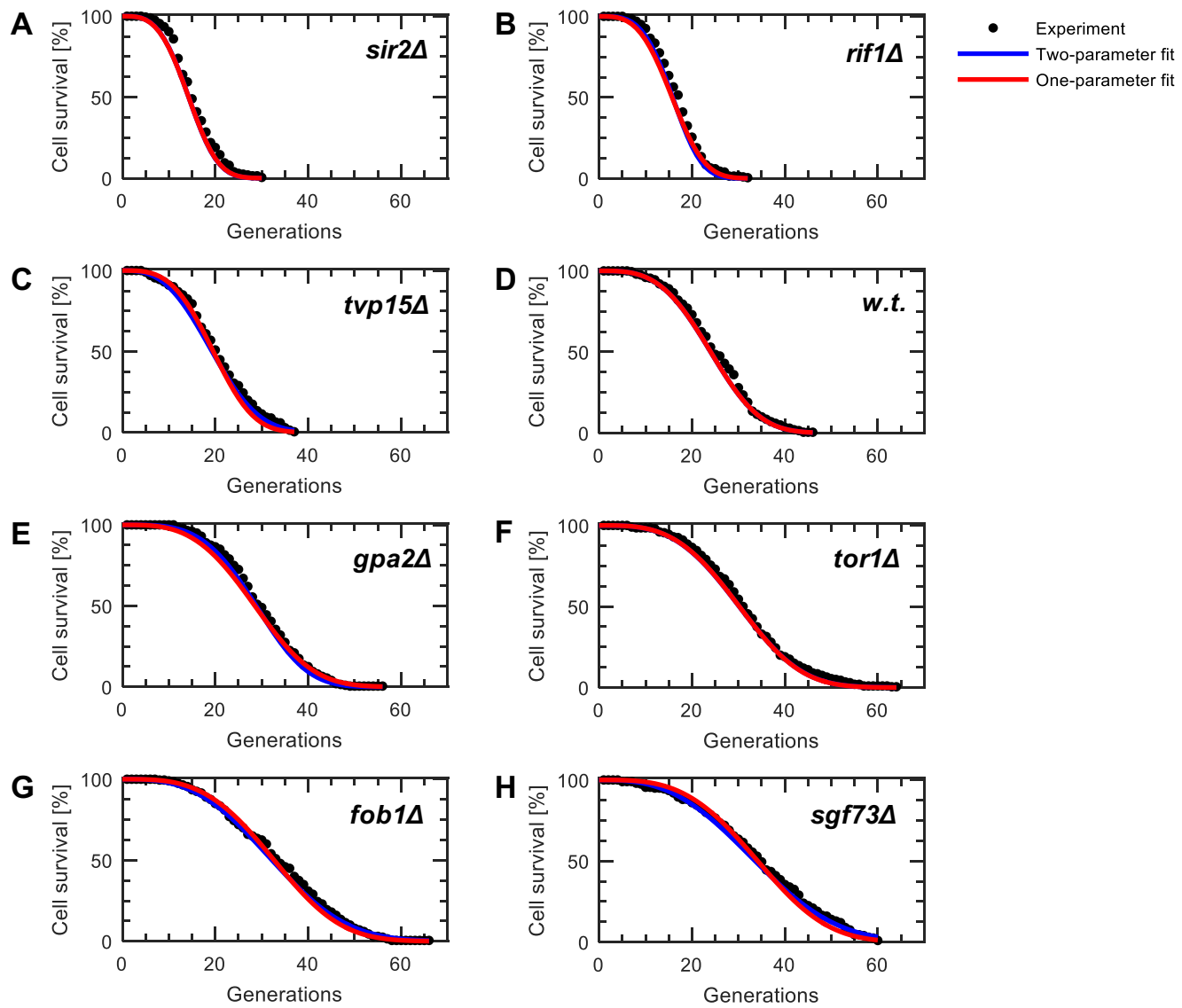


Figure S3

**fig. S3. Fit performance comparisons between one- and two-parameter Weibull survival functions. A-H.** Experimental cell survival data (black dots) from eight different strains were fitted with one or two-parameter Weibull survival functions (red or blue lines, respectively) using the least-squares fitting approach. N=200 cells were analyzed from each strain. Strain names are indicated on each panel (*w.t.*: wild-type;  $\Delta$ : gene deletion). For one-parameter Weibull survival function fit,  $\alpha$  was set to 3.28, corresponding to the value of  $\alpha$  extracted from the two-parameter Weibull survival function fit using N=200 wild type cells.



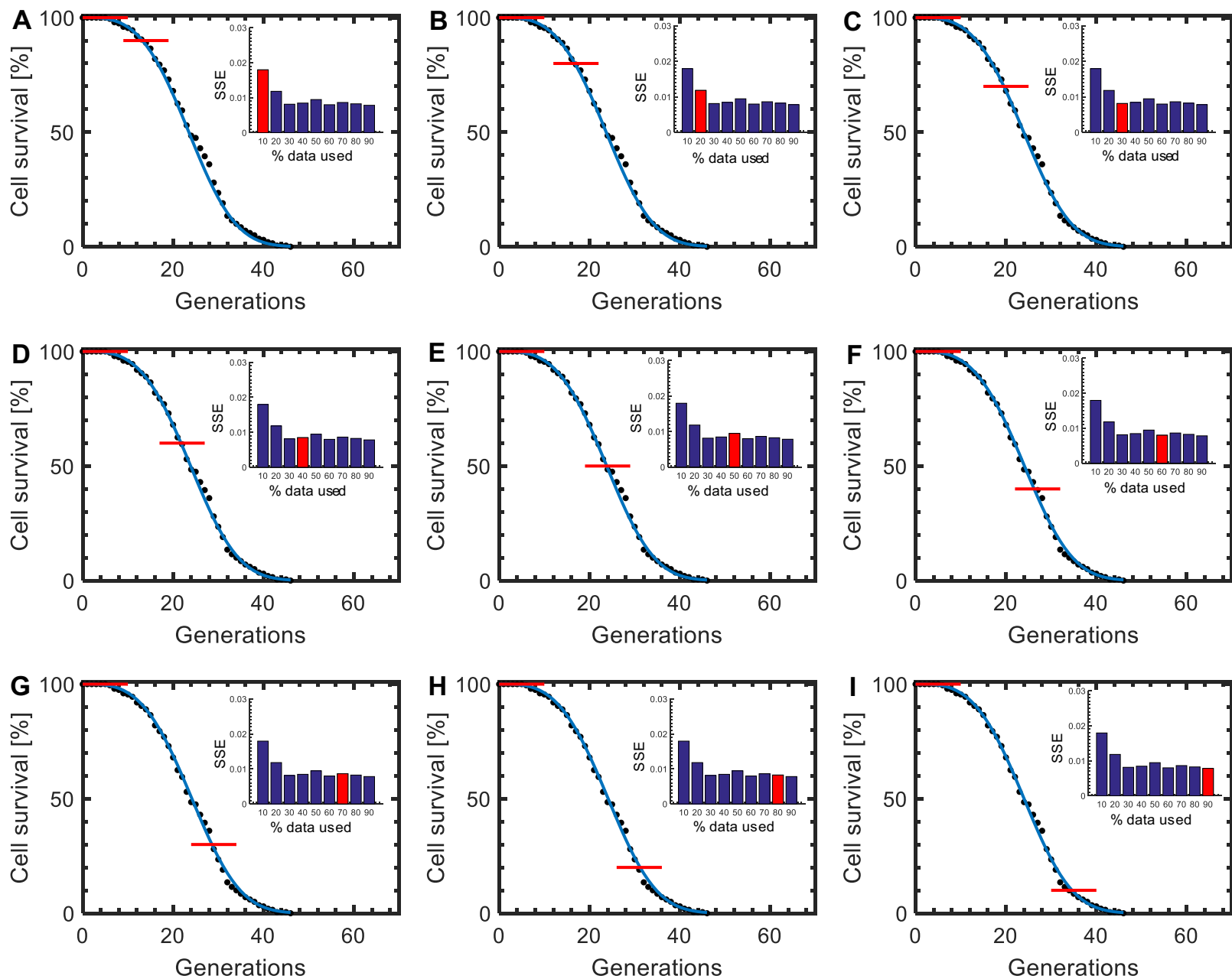


Figure S4

**fig. S4. Predictive capacity characterization for the one-parameter Weibull survival function on 200 wild-type cells.** The wild type cell survival curve (black) was split into nine portions covering from 10% (A) to 90% (I) of the cell survival data as indicated by the red lines. Each portion was separately used in the fitting process and the best-fitting value of the scaling parameter  $r$  was fed into the one-parameter Weibull survival function to predict the entire cell survival distribution (blue). The insets show the SSE values (sum of squared errors between black points and blue curve) obtained after using each portion (red) of the data. The SSE values approximately flat line starting at 30% of the data used. N=200 wild type cells. For one-parameter Weibull survival function fits,  $\alpha$  was set to 3.28, corresponding to the value of  $\alpha$  extracted from the two-parameter Weibull survival function fit using N=200 wild type cells.

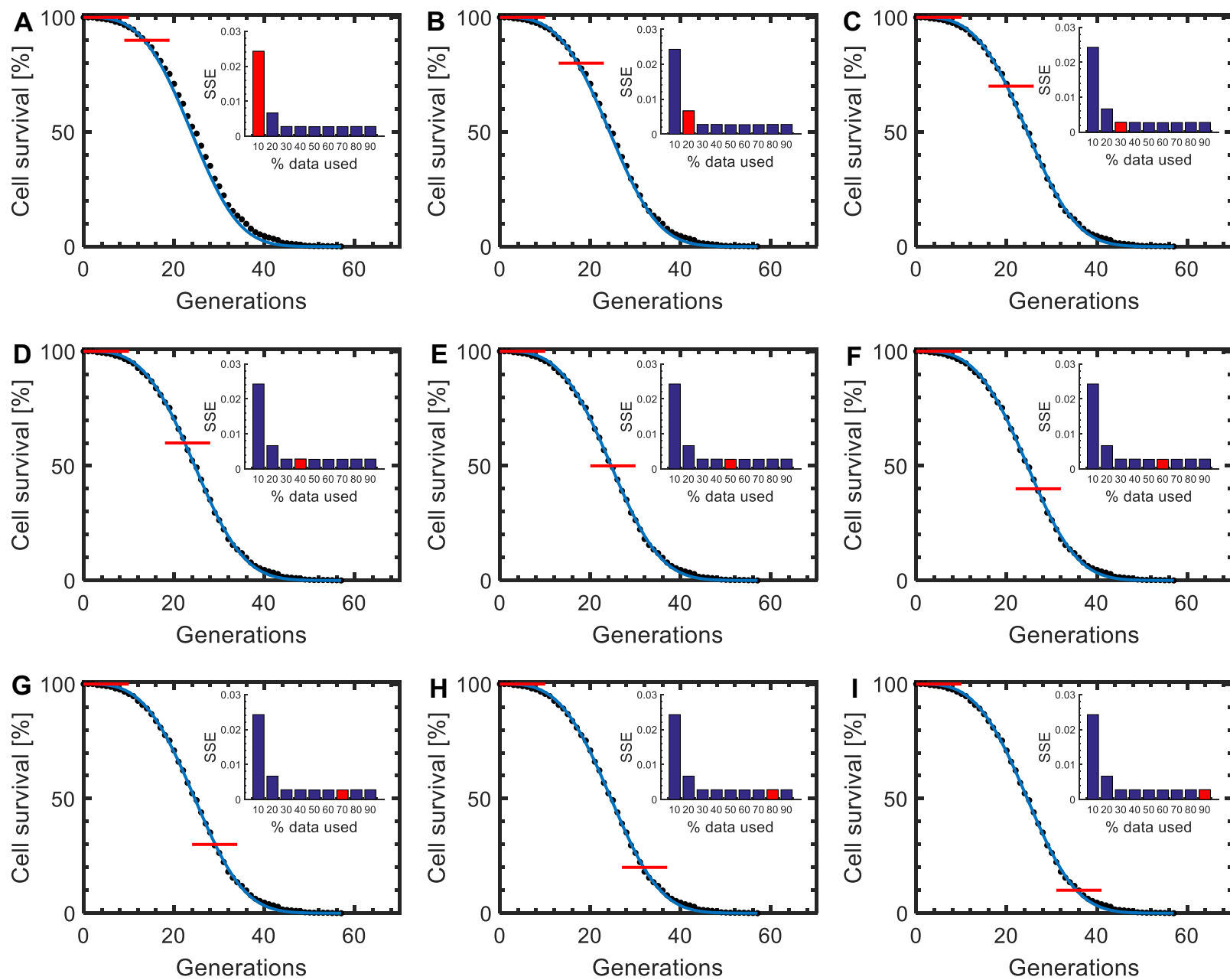
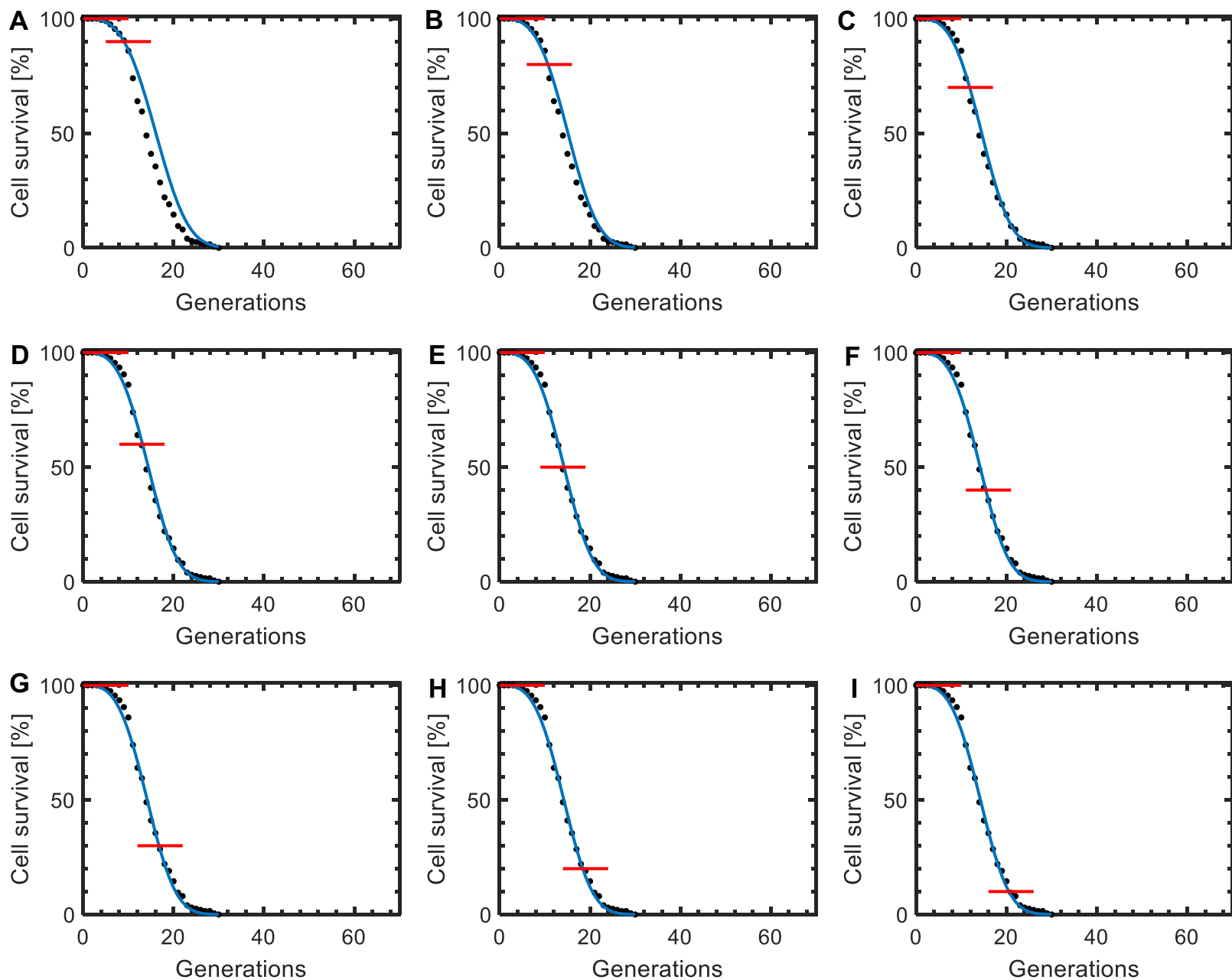


Figure S5

**fig. S5. Predictive capacity characterization for the one-parameter Weibull survival function on 1000 wild-type cells.** The wild type cell survival curve (black) was split into nine portions covering from 10% (A) to 90% (I) of the cell survival data as indicated by the red lines. Each portion was separately used in the fitting process and the best-fitting value of the scaling parameter  $r$  was fed into the one-parameter Weibull survival function to predict the entire cell survival distribution (blue). The insets show the SSE values (sum of squared errors between black points and blue curve) obtained after using each portion (red) of the data. The SSE values approximately flat line starting at 30% of the data used. N=1000 wild type cells.



**Figure S6** (*sir2Δ*)

**fig. S6. Predictive capacity characterization for the one-parameter Weibull survival function on *sir2Δ*.** The *sir2Δ* cell survival curve (black) was split into nine portions covering from 10% (A) to 90% (I) of the cell survival data as indicated by the red lines. Each portion was separately used in the fitting process and the resulting best-fitting parameter values were used to predict the entire cell survival distribution (blue). N=200 cells.

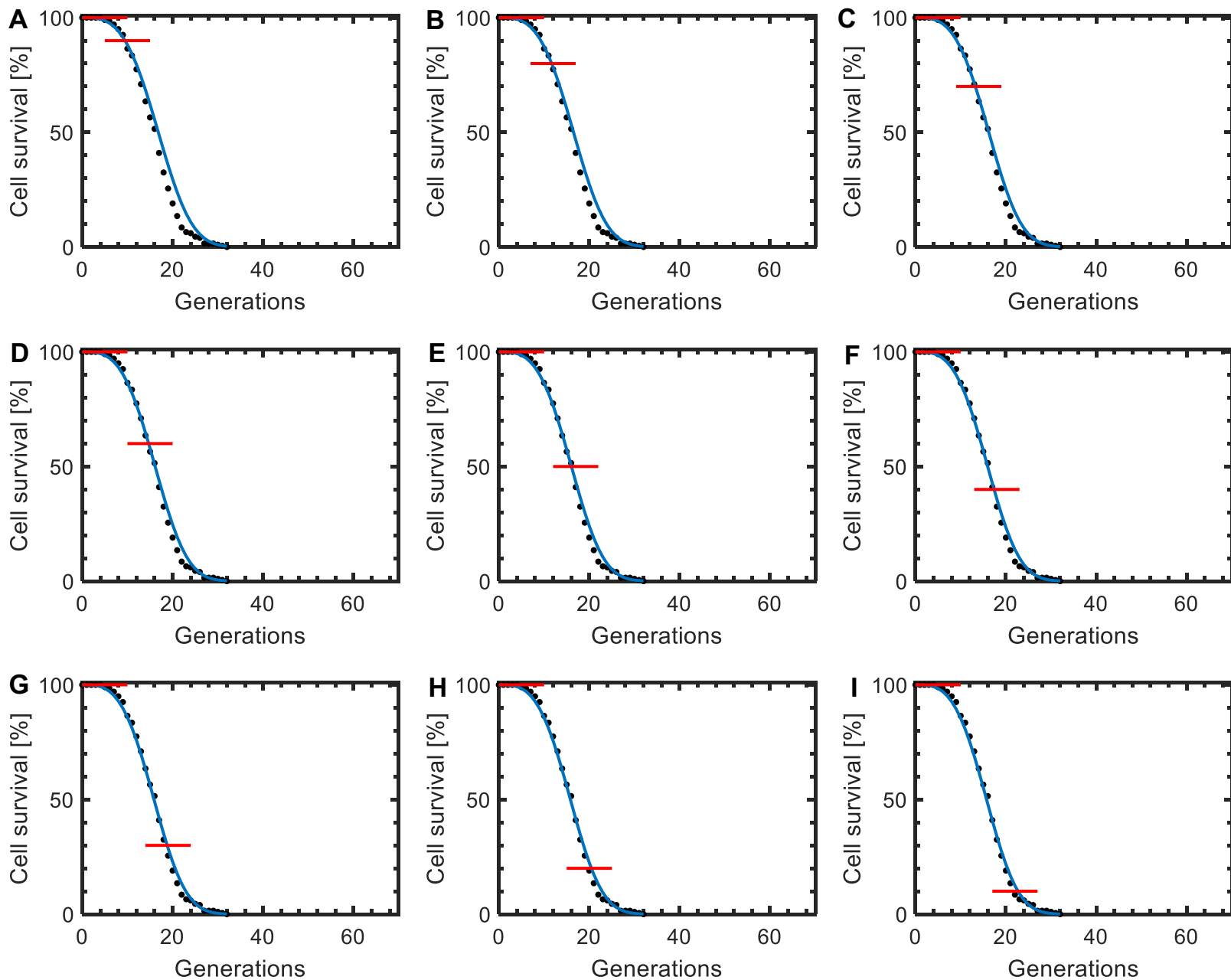


Figure S7 (*rif1Δ*)

**fig. S7. Predictive capacity characterization for the one-parameter Weibull survival function on *rif1*Δ.** The *rif1*Δ cell survival curve (black) was split into nine portions covering from 10% (A) to 90% (I) of the cell survival data as indicated by the red lines. Each portion was separately used in the fitting process and the resulting best-fitting parameter values were used to predict the entire cell survival distribution (blue). N=200 cells.



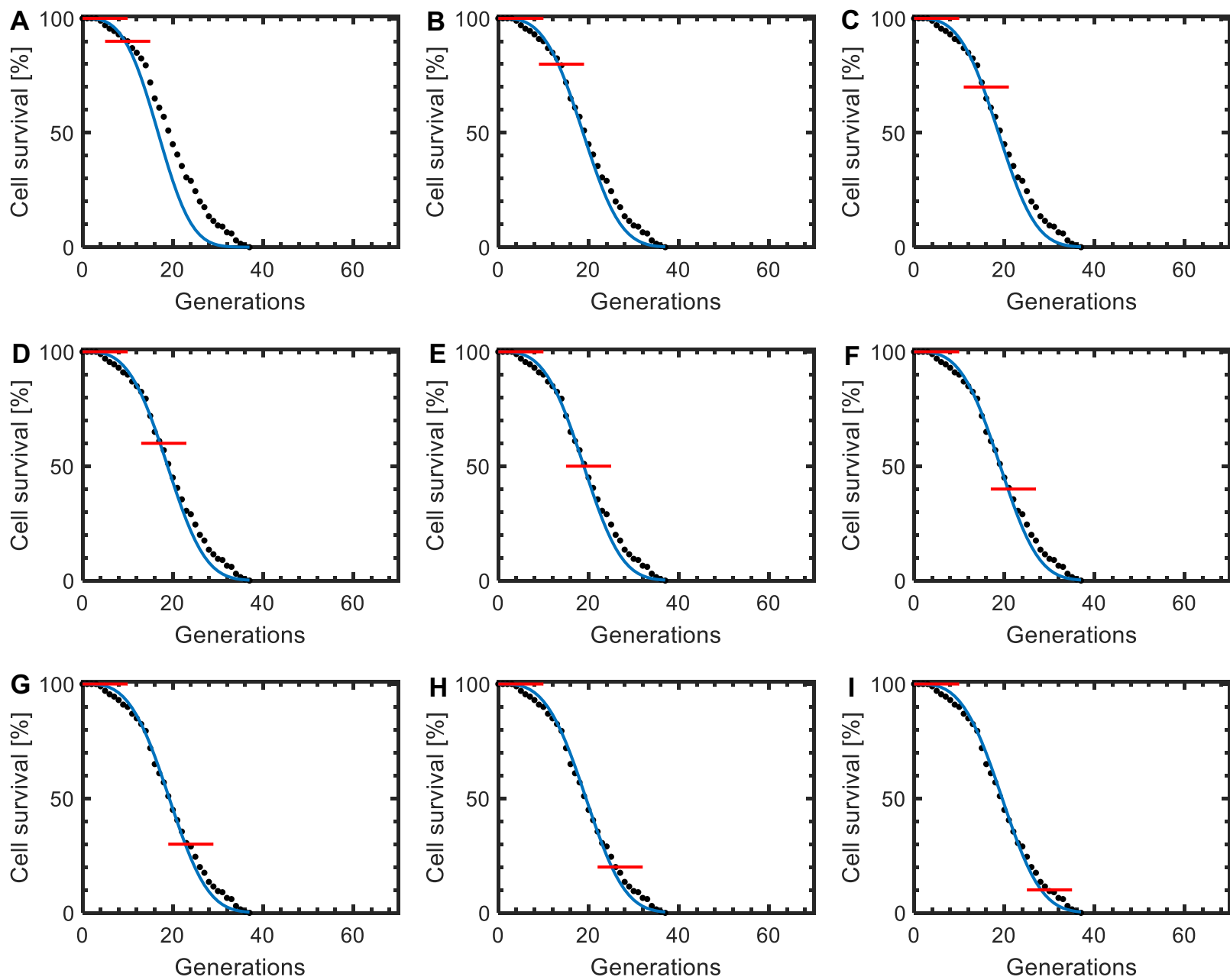


Figure S8 (*tvp15Δ*)

**fig. S8. Predictive capacity characterization for the one-parameter Weibull survival function on *tpv15Δ*.** The *tpv15Δ* cell survival curve (black) was split into nine portions covering from 10% (A) to 90% (I) of the cell survival data as indicated by the red lines. Each portion was separately used in the fitting process and the resulting best-fitting parameter values were used to predict the entire cell survival distribution (blue). N=200 cells.

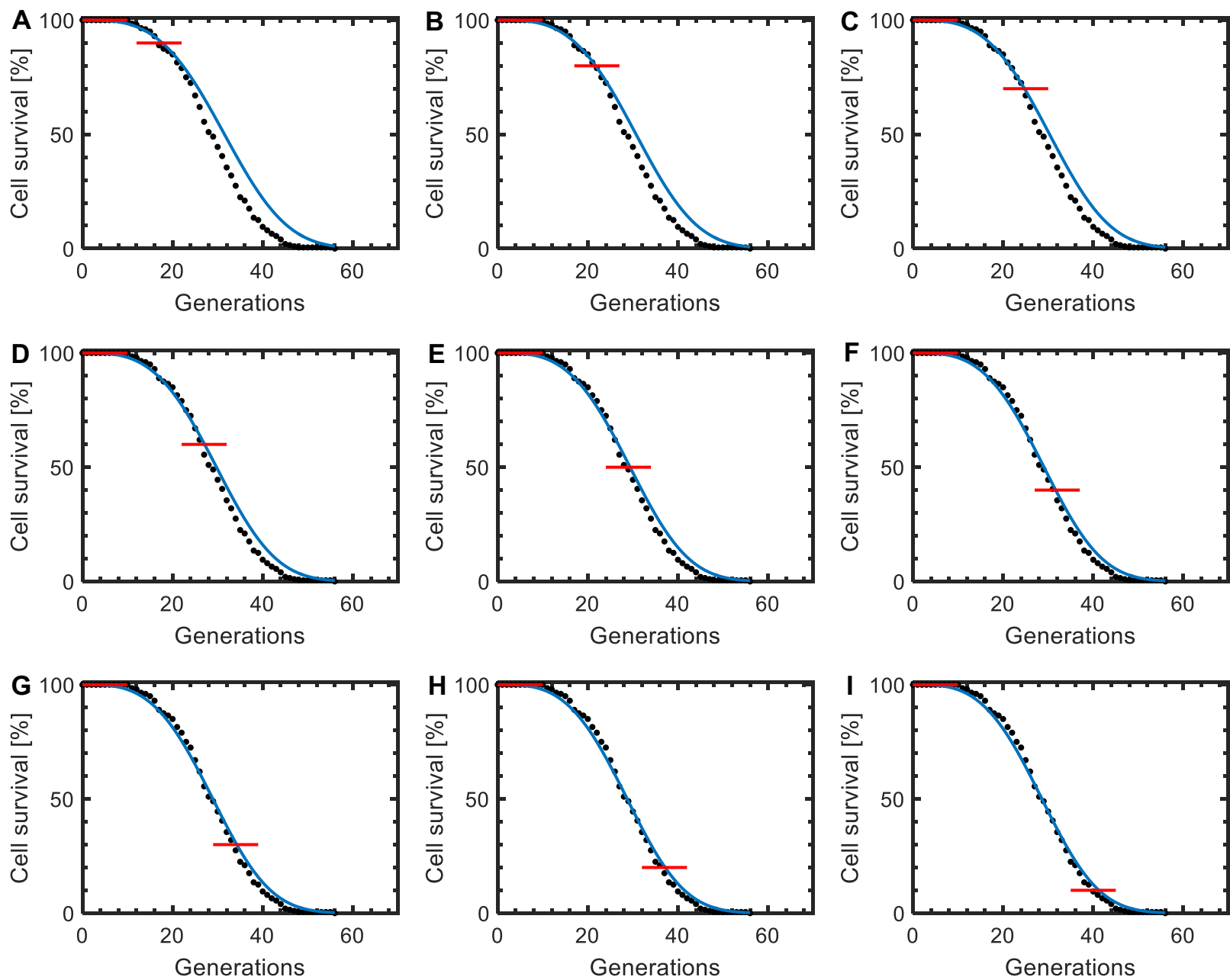
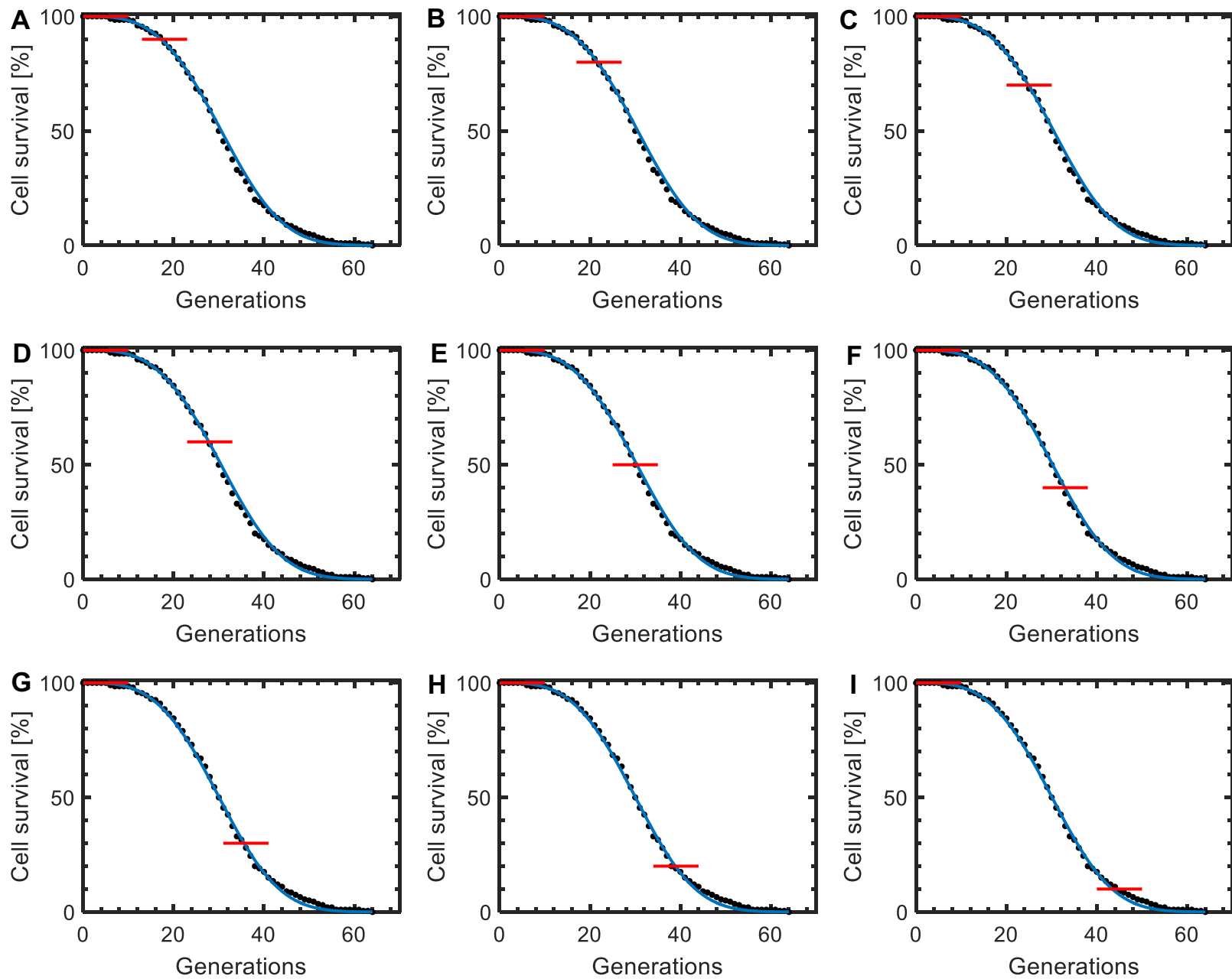


Figure S9 (*gpa2Δ*)

**fig. S9. Predictive capacity characterization for the one-parameter Weibull survival function on *gpa2Δ*.** The *gpa2Δ* cell survival curve (black) was split into nine portions covering from 10% (A) to 90% (I) of the cell survival data as indicated by the red lines. Each portion was separately used in the fitting process and the resulting best-fitting parameter values were used to predict the entire cell survival distribution (blue). N=200 cells.



**Figure S10** (*tor1Δ*)

**fig. S10. Predictive capacity characterization for the one-parameter Weibull survival function on *tor1Δ*.** The *tor1Δ* cell survival curve (black) was split into nine portions covering from 10% (A) to 90% (I) of the cell survival data as indicated by the red lines. Each portion was separately used in the fitting process and the resulting best-fitting parameter values were used to predict the entire cell survival distribution (blue). N=200 cells.

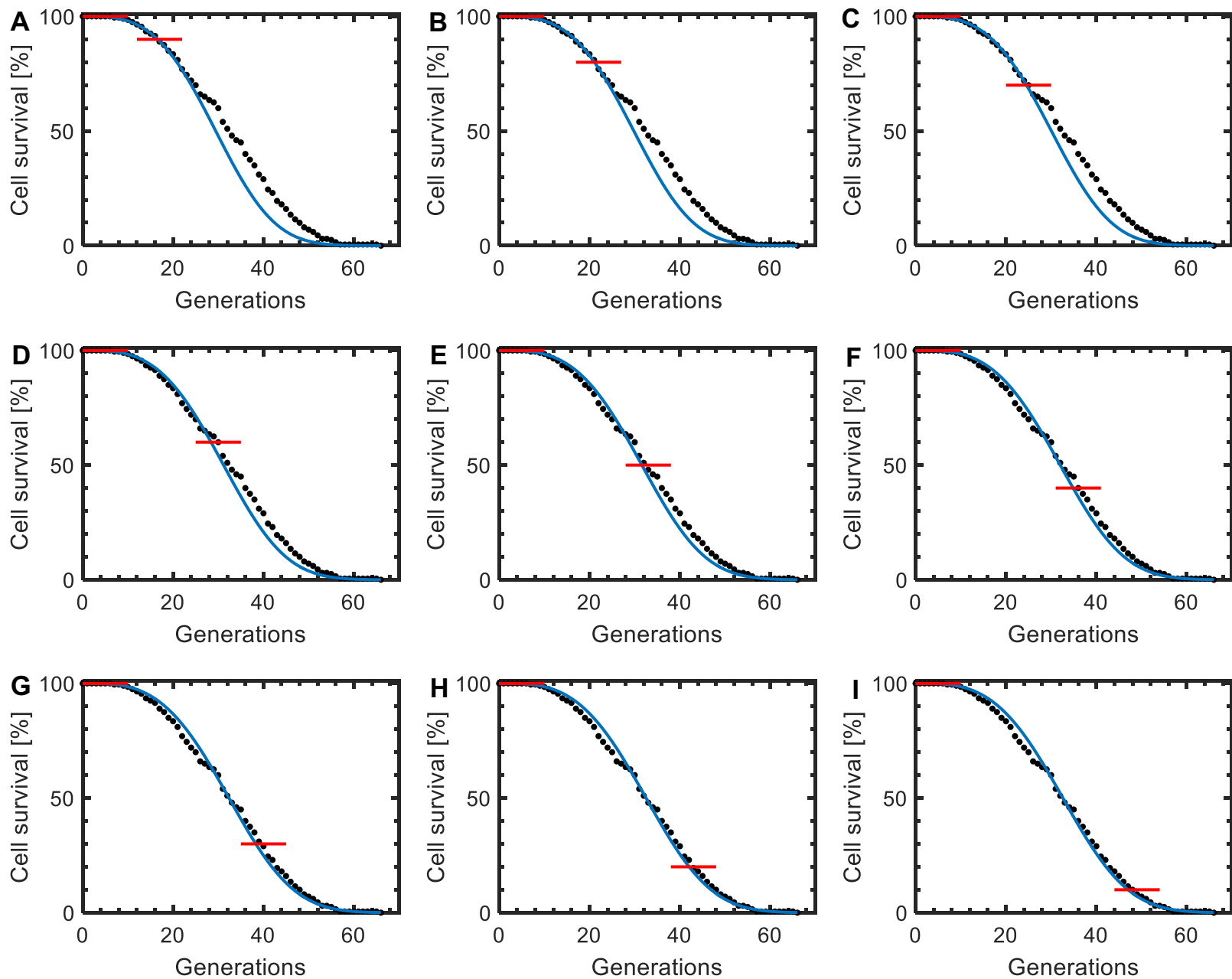


Figure S11 (*fob1Δ*)

**fig. S11. Predictive capacity characterization for the one-parameter Weibull survival function on *fob1Δ*.** The *fob1Δ* cell survival curve (black) was split into nine portions covering from 10% (A) to 90% (I) of the cell survival data as indicated by the red lines. Each portion was separately used in the fitting process and the resulting best-fitting parameter values were used to predict the entire cell survival distribution (blue). N=200 cells.



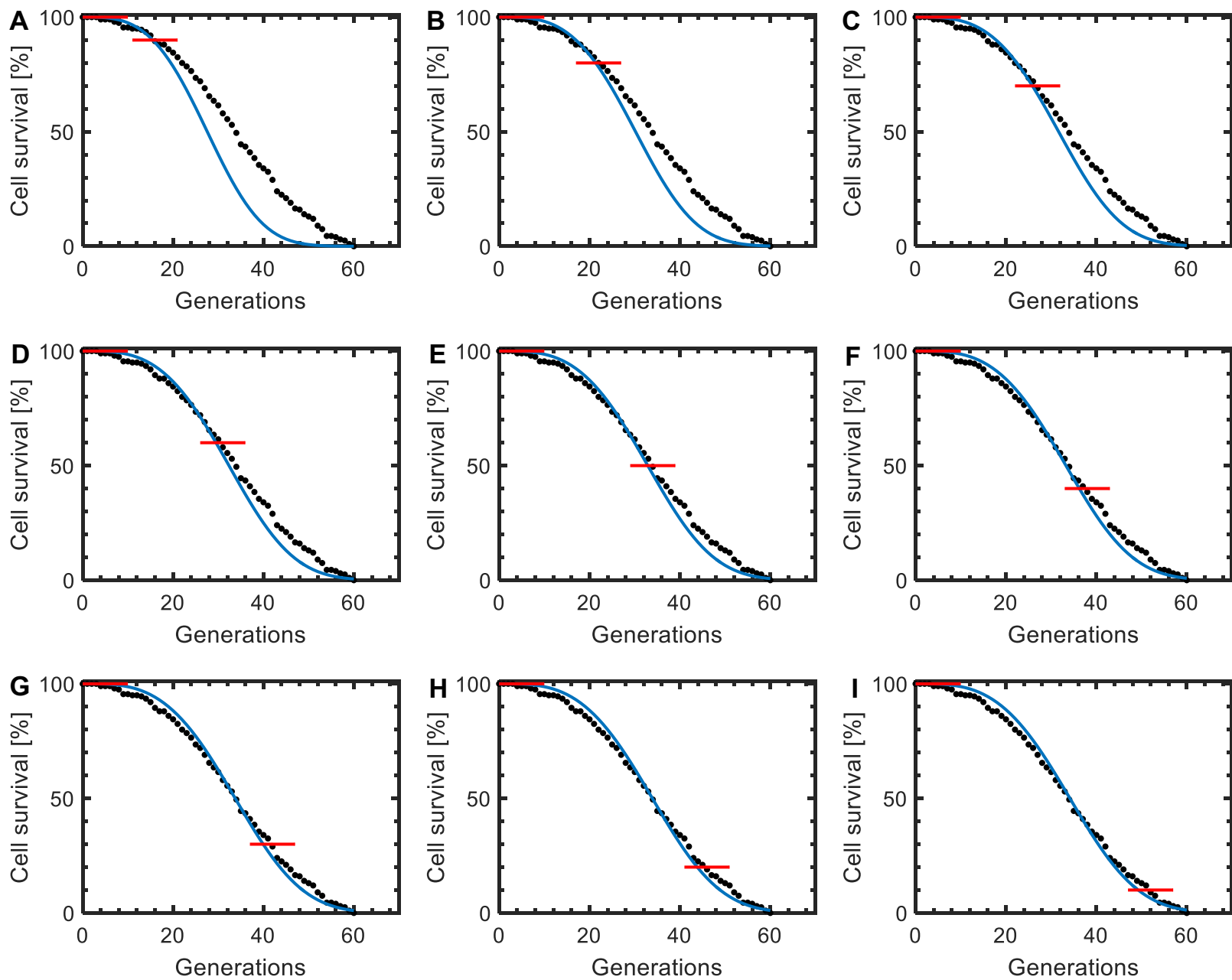


Figure S12 (*sgf73Δ*)

**fig. S12. Predictive capacity characterization for the one-parameter Weibull survival function on *sgf73Δ*.** The *sgf73Δ* cell survival curve (black) was split into nine portions covering from 10% (A) to 90% (I) of the cell survival data as indicated by the red lines. Each portion was separately used in the fitting process and the resulting best-fitting parameter values were used to predict the entire cell survival distribution (blue). N=200 cells.

## II. SUPPLEMENTARY TABLES

Strain	<i>rif1Δ</i>	<i>tvp15Δ</i>	<i>w.t.</i>	<i>gpa2Δ</i>	<i>tor1Δ</i>	<i>fob1Δ</i>	<i>sgf73Δ</i>
<i>sir2Δ</i>	0.105	0.120	0.120	0.110	0.100	0.115	0.145
<i>rif1Δ</i>	NA	0.160	0.105	0.070	0.070	0.125	0.155
<i>tvp15Δ</i>	NA	NA	0.110	0.155	0.105	0.080	0.080
<i>w.t.</i>	NA	NA	NA	0.135	0.100	0.095	0.135
<i>gpa2Δ</i>	NA	NA	NA	NA	0.080	0.125	0.160
<i>tor1Δ</i>	NA	NA	NA	NA	NA	0.120	0.140
<i>fob1Δ</i>	NA	NA	NA	NA	NA	NA	0.080

table S1. Results from the Kolmogorov-Smirnov statistic  $\sup|S_i - S_j|$ , where  $\sup$  is the supremum (maximum) function.

Strain	<i>rif1Δ</i>	<i>tvp15Δ</i>	<i>w.t.</i>	<i>gpa2Δ</i>	<i>tor1Δ</i>	<i>fob1Δ</i>	<i>sgf73Δ</i>
<i>sir2Δ</i>	0.220	0.112	0.112	0.178	0.270	0.142	0.030
<i>rif1Δ</i>	NA	0.012	0.220	0.711	0.711	0.088	0.016
<i>tvp15Δ</i>	NA	NA	0.178	0.016	0.220	0.544	0.544
<i>w.t.</i>	NA	NA	NA	0.052	0.270	0.327	0.052
<i>gpa2Δ</i>	NA	NA	NA	NA	0.544	0.088	0.012
<i>tor1Δ</i>	NA	NA	NA	NA	NA	0.112	0.040
<i>fob1Δ</i>	NA	NA	NA	NA	NA	NA	0.544

table S2. P values computed using *ks.test* function of R.

	$\alpha$	r	SSE	R-square
Gompertz	0.0037	0.132	0.0213	0.9969
Gamma	8.52	0.348	0.0276	0.9960
Weibull	3.28	0.0372	0.0078	0.9989

table S3. Fit results from the use of the two-parameter Gompertz,  $\gamma$ , and Weibull survival functions. 100% of the cell viability data was used in the fit. N=200 wild-type cells.

Strain	$\alpha$	r	SSE	R-square
<i>sir2Δ</i>	3.31	0.0627	0.0127	0.9974
<i>rif1Δ</i>	3.64	0.0571	0.0035	0.9993
<i>tpv15Δ</i>	2.82	0.0455	0.0062	0.9987
<i>w.t.</i>	3.28	0.0372	0.0078	0.9989
<i>gpa2Δ</i>	3.75	0.0315	0.0039	0.9996
<i>tor1Δ</i>	3.26	0.0296	0.0093	0.9991
<i>fob1Δ</i>	2.91	0.0273	0.0120	0.9988
<i>sgf73Δ</i>	2.78	0.0261	0.0089	0.9988

**table S4. Fit performance of the two-parameter Weibull survival function.** 100% of the cell viability data was used in the fit. N=200 cells.

Strain	r	SSE	R-square
<i>rif1Δ</i>	0.0627	0.0128	0.9973
<i>tpv15Δ</i>	0.0569	0.0103	0.9980
<i>sir2Δ</i>	0.0457	0.0261	0.9947
<i>w.t.</i>	0.0372	0.0078	0.9989
<i>sgf73Δ</i>	0.0313	0.0249	0.9973
<i>tor1Δ</i>	0.0296	0.0094	0.9991
<i>gpa2Δ</i>	0.0274	0.0338	0.9965
<i>fob1Δ</i>	0.0262	0.0501	0.9931

**table S5. Fit performance of the one-parameter Weibull survival function ( $\alpha$  is fixed at 3.28).** 100% of the cell viability data was used in the fit. N=200 cells.

% viability	r	SSE	R-square
10%	0.0381	0.0179	0.9975
20%	0.0378	0.0118	0.9983
30%	0.0374	0.0081	0.9989
40%	0.0374	0.0085	0.9988
50%	0.0376	0.0095	0.9987
60%	0.0371	0.0080	0.9989
70%	0.0370	0.0086	0.9988
80%	0.0371	0.0083	0.9988
90%	0.0373	0.0078	0.9989

**table S6. Fit and prediction results from the use of the one-parameter Weibull survival function.** The indicated % of the cell viability data was used in the fit, which resulted in the specific r values shown. Then, the entire survival curve was predicted using each specific r value in the one-parameter Weibull survival function ( $\alpha$  is fixed at 3.28), and the SSE and R-square values were calculated based on the full survival curve predicted. N=200 wild type cells.

% viability	r	SSE	R-square
10%	0.0375	0.0243	0.9974
20%	0.0368	0.0066	0.9993
30%	0.0364	0.0028	0.9997
40%	0.0364	0.0028	0.9997
50%	0.0363	0.0027	0.9997
60%	0.0363	0.0027	0.9997
70%	0.0363	0.0027	0.9997
80%	0.0364	0.0028	0.9997
90%	0.0364	0.0028	0.9997

**table S7. Fit and prediction results from the use of the one-parameter Weibull survival function.**

The indicated % of the cell viability data was used in the fit, which resulted in the specific r values shown. Then, the entire survival curve was predicted using each specific r value in the one-parameter Weibull survival function ( $\alpha$  is fixed at 3.28), and the SSE and R-square values were calculated based on the full survival curve predicted. N=1000 wild type cells.

Strain	Genotype
AL001	<i>MATa, his3Δ, leu2Δ, ura3Δ, lys2Δ</i>
<i>sir2Δ</i>	<i>MATa, his3Δ, leu2Δ, ura3Δ, met15Δ, sir2Δ</i>
<i>rif1Δ</i>	<i>MATa, his3Δ, leu2Δ, ura3Δ, met15Δ, rif1Δ</i>
<i>tpv15Δ</i>	<i>MATa, his3Δ, leu2Δ, ura3Δ, met15Δ, tpv15Δ</i>
<i>sgf73Δ</i>	<i>MATa, his3Δ, leu2Δ, ura3Δ, met15Δ, sgf73Δ</i>
<i>tor1Δ</i>	<i>MATa, his3Δ, leu2Δ, ura3Δ, met15Δ, tor1Δ</i>
<i>gpa2Δ</i>	<i>MATa, his3Δ, leu2Δ, ura3Δ, met15Δ, gpa2Δ</i>
<i>fob1Δ</i>	<i>MATa, his3Δ, leu2Δ, ura3Δ, met15Δ, fob1Δ</i>

**table S8. Yeast strains used in this study.** All *S. cerevisiae* strains used have the BY genetic background. The strain AL001 has the wild type background.

## Supplementary Materials and Methods

### Accelerated Failure Time (AFT) Model

The mathematical form  $S_1(g) = S_2(\lambda^{-1}g)$  indicating the invariance of a survival function with respect to the variable of generations is known as an Accelerated Failure Time (AFT) model. The generational variable  $g$  of the first distribution  $S_1$  corresponding to the genetic background 1 can be linearly transformed into the value  $\lambda^{-1}g$  of the second distribution  $S_2$  corresponding to the genetic background 2. An AFT regression model with a single categorical covariate can be formulated as

$$\log g_i = \beta x_i + \varepsilon_i$$

where  $g_i$  is the lifespan of cell  $i$ ;  $x_i$  is a vector encoding the value of an explanatory categorical variable  $X$  for cell  $i$ ;  $\beta$  is the parameter vector to be estimated;  $\varepsilon_i$  is a residual representing the logarithm of the lifespan of cell  $i$  unexplained by the covariate. The relation to the scale factor  $\lambda$  is given by  $\lambda = \exp(\beta x_i)$ . The AFT model is applied here to link genetic interventions in aging to their quantitative impact on replicative lifespan. When the AFT model provides a fit across multiple lifespan distributions, then the interventions leading to the lifespan distributions result in generational scaling. The presence of generational scaling suggests that the genetic interventions change the lifespan by changing the timescale of a key aging process that determines the risk of cell death. In addition to the accelerated failure time model, a second formalism (proportional hazards) also exists. However, if the cell survival statistics follow a Weibull distribution (which is the case for the replicative aging of yeast cells, as shown in this study), the two formalisms are mathematically equivalent. We estimated the parameters from the AFT model by performing regression analysis using MATLAB. Each time the AFT regression was run, the intercept determining the reference replicative lifespan (in relation to which the parameter vector  $\beta$  was scaled) was set at 3.09 which was computed based on the data from 200 wild type cells.

### Quantifying generational scaling

We quantified deviations from generational scaling by applying a Kolmogorov-Smirnov (KS) test (3, 18) to the residuals of the AFT regression model. The KS test tested whether the AFT residuals came from the same distribution, which would correspond to that all statistical differences between two sets of lifespan data could indeed be accounted for by a scale factor, leading to the conclusion that the two distributions were related by generational scaling. The KS test also served as a distance metric between two survival curves.

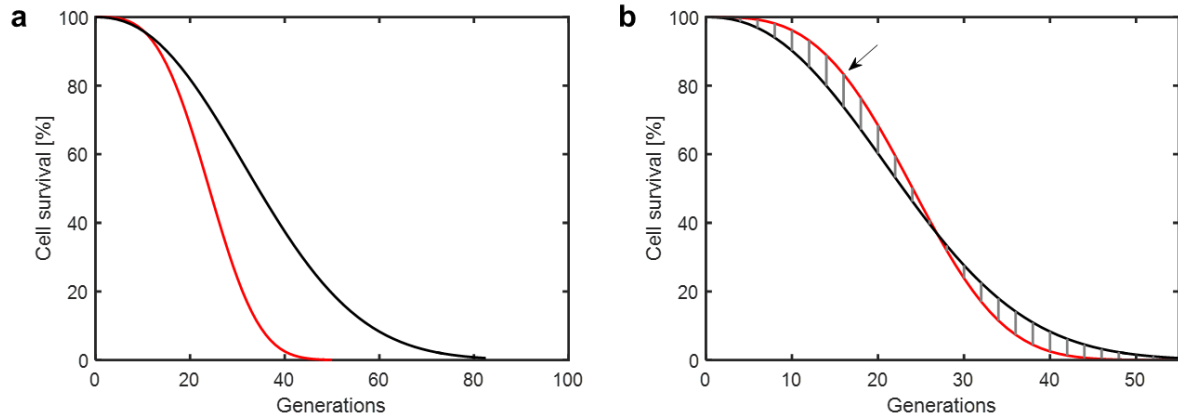


**fig. S13. Quantifying deviations from perfect scaling.** **a.** Sample survival curves for two yeast strains before applying the Accelerated Failure Time (AFT) model. **b.** After the AFT model has been applied using the red survival curve (**a**) as the reference, maximum difference (arrow) between the two resulting scaled curves is quantified using KS test to evaluate deviation from perfect scaling.

Using the survival data for a pair of survival curves  $S_1(g)$  and  $S_2(g)$  to be compared for a potential scale invariance, we first fit the two data sets to the AFT regression model, extract the parameter vector  $\beta$ , and obtain the scaled versions of the two curves. We next quantify the difference between the two scaled curves

$$F_{1,2}(g) = S_1(g) - S_2(g)$$

and calculate the KS statistic  $D_{1,2}$  by taking the maximum value of  $F_{1,2}(g)$

$$D_{1,2} = \sup |F_{1,2}(g)|$$

$D_{1,2}$  is used to calculate a p-value related to the null hypothesis which, after the AFT scaling, affirms generational scaling. Obtained using the `ks.test` package of R, a low p-value would suggest a significant deviation from perfect scaling between the two scaled survival curves being compared. For significance determination, we performed 28 pairwise comparisons between the 8 strains. All p-values resulting from the application of the KS test were higher than 0.0018 (table S2). This pairwise p-value threshold of 0.0018 ( $=0.05/28$ ) corresponds to the significance level of 0.05 for the family of 28 pairwise comparisons using Bonferroni's correction method for multiple hypothesis testing. The  $D_{1,2}$  values calculated were also low across the board (table S1) indicating the closeness between any two scaled survival curves.

To evaluate the sensitivity of the KS test after the application of the AFT model, we compared sets of simulated replicative lifespan distributions (fig. S1), each of which was obtained by using a specific value of the Weibull  $\alpha$  parameter. Using populations of 1000 cells, the KS test statistic reliably identified changes in the Weibull  $\alpha$  parameter of  $\sim 1$ .

To assess the statistical power of the test, we generated sets of simulated lifespans as for figure S1B, but varied the population size between 50 and 6776 cells (fig. S1C). The Weibull  $\alpha$  parameter was varied between 0.33 and 8.13. Populations corresponding to each parameter set were compared to a baseline population of equal size with a Weibull  $\alpha$  value equal to 3.28 which was chosen based on the Weibull  $\alpha$  value observed from the wild type yeast replicative lifespan distribution. The p-value from each comparison was collected across 1000 replicates. For each set of replicates and each population size, the fraction of insignificant p-values ( $\geq 0.0018$ ) was then calculated to estimate the power of the KS test at each population size. figure S1D shows the  $\alpha$  values that can be detected at given population sizes with a given false negative rate. The false negative rates we included in the analysis ranged from 0.01 (1% of all true deviations from survival curve shape are missed) to 0.5 (half of all true deviations from survival curve shape are missed). Substantial increases in population size were required to achieve relatively higher statistical power.

### Parametric description of cell survival distributions

To find out a functional form that can mathematically describe the experimental survival dynamics, we tested three probability distributions (gamma, Gompertz and Weibull) that have been historically (13-16) used to describe morbidity statistics of living systems. These distributions, each defined by two parameters, are described by the following survival functions

$$\text{Gamma } (r, \alpha): \quad \frac{S}{S_0} = \frac{r^\alpha}{\Gamma(\alpha)} \int_g^\infty t^{\alpha-1} e^{-rt} dt$$

$$\text{Gompertz } (r, \alpha): \quad \frac{S}{S_0} = e^{\frac{\alpha}{r}(1-e^{rg})}$$

$$\text{Weibull } (r, \alpha): \quad \frac{S}{S_0} = e^{-(rg)^\alpha}$$

In these equations,  $g$  describes the dimensionless replicative age of a cell ( $g = G/G_0$ , where  $G$  is the actual replicative age of a cell and  $G_0$  is the scaling constant which has the fixed value of 1 generation),  $S$  is the number of cells that are alive at generation  $G$ , and  $S_0$  is the initial number of cells to be followed during their aging process. Here we experimentally and computationally analyze the generation-specific cell survival values ( $S/S_0$ ).

Using the survival models described above, we performed three separate least-squares fits between each model and the experimental survival profile of the wild type yeast cells (Fig. 1D). The choices for the initial values of the two parameters were made based on values used in literature (13). The reliability of the fits was further confirmed by systematically sampling different values of the two parameters from large ranges (fig. S2). The two-parameter Weibull distribution emerged as the distribution providing the best fit to the data (Fig. 3, table S3).

Another layer of support for identifying the Weibull distribution as a precise parametric form to use to describe the experimental survival dynamics of yeast cells comes from a comparative



inspection of the forms of the two-parameter gamma, Gompertz, and Weibull survival functions. In order for a function to fulfill the experimentally observed generational scalability requirement, the parameter next to the generational variable  $g$  should always occur next to the variable  $g$  whenever it is present in the functional form. The parameter  $r$  of the two-parameter Weibull survival function satisfies this requirement while the forms of the gamma and Gompertz survival functions do not.

We next wanted to see how the one-parameter version of the Weibull survival function (with  $r$  being the only parameter) would perform in comparison to its two-parameter version. For this, we fixed the value of  $\alpha$  to 3.28 which corresponds to the value obtained from fitting the wild type survival data to the two-parameter Weibull survival function (table S3). Then, using custom-written MATLAB scripts for least-squares fitting and generating fit statistics, we performed separate fits between: (i) the two-parameter Weibull survival function and the survival distribution of each of the 8 strains including the wild type (table S4), and (ii) the one-parameter Weibull survival function and the survival distribution of each of the 8 strains including the wild type (table S5). The cost function was obtained by summing the squared differences between the function-produced cell survival values and the experimentally-obtained ones and it was minimized (separately for each strain) by using the fit parameter(s). Supplementary Tables S4-S5 provide the best-fitting parameter values as well as other fit statistics. As can be seen from the resulting parameter values, the strain-specific values of the scaling parameter  $r$  were very similar between the two-parameter and one-parameter Weibull fitting, validating fixing the value of  $\alpha$  at 3.28. This analysis shows that the one-parameter Weibull survival function  $S/S_0 = e^{-(rg)^{3.28}}$  can be used as a scalable precise parametric form to describe the experimental survival dynamics of yeast cells.

#### **IV. Investigation of stochastic models describing aging at the microscopic level**

In this section, we evaluate multiple specific stochastic processes that are often used (3, 19) to study aging at microscopic level: semi-infinite random walk, drift-diffusion process with drift heterogeneity, and Strehler-Mildvan model with vitality drift-diffusion. Importantly, the survival functions corresponding to these models satisfy the scalability requirement (3). We tested the suitability of these models for describing our data by exploring a wide range of parameter space for each individual model and then by comparing the simulated survival curves to the one we obtained experimentally from the wild type yeast cells.

##### **i. Semi-infinite random walk**

A stochastic variable  $X(t)$  continuous in time  $t$  is used to track the aging of a single cell microscopically. Before the random walk process starts, the variable is assigned a random discrete state  $i$ :  $X(0) = i$ , with  $i = 0, 1, 2, \dots$ . The random walker then moves 1 step upward or downward depending on the governing rate constants  $\beta^+$  and  $\beta^-$ . Whenever the random walker reaches the boundary at 0, the process stops and the random walker is considered dead. The

elapsed time is then recorded as the replicative lifespan of the simulated cell. The corresponding survival function  $S(t)$  is given (3) by

$$S(t) = 1 - i \left( \frac{\beta^-}{\beta^+} \right)^{\frac{i}{2}} \int_0^t \frac{1}{\tau} \exp(-(\beta^- + \beta^+) \tau) I_i(2\sqrt{\beta^- \beta^+} \tau) d\tau, \quad (1)$$

where  $I_i(x)$  is the modified Bessel function (of the first kind) of order  $i$ .

## ii. Drift-diffusion process with drift heterogeneity

In this case, the stochastic variable  $X(t)$  moves in continuous state space following a drift-diffusion process with initial state  $c$

$$X(t) = c - \mu t + \sigma W(t) \quad (2)$$

where  $\mu$  and  $\sigma^2$  represent the drift and diffusion coefficients respectively. Drift  $\mu$  is constrained to have a positive value here to reflect the fact that the vitality state has a general decreasing trend.  $W(t)$  denotes a Wiener process, with  $W(0) = 0$ . The Wiener process has independent increments,  $W(t+u)-W(t)$  is independent of  $W(s)$  for all  $s \leq t$  and  $u \geq 0$ . The increments are normally distributed,  $W(t+u)-W(t) \sim N(0, u)$ . Lastly, the Wiener process is continuous in time. To introduce more flexibility, we allow the drift coefficient to have heterogeneity and to be chosen from a normal distribution with mean  $\mu_{mean}$  and standard deviation  $\mu_{sd}$ . For this drift-diffusion process with drift heterogeneity and initial condition  $X(0) = c$ , its corresponding survival function  $S(t)$  is given (3) by

$$S(t) = \phi \left( \frac{c - \mu_{mean} t}{\sqrt{t(\sigma^2 + t\mu_{sd}^2)}} \right) - \phi \left( -\frac{c\sigma^2 + t\mu_{mean}\sigma^2 + 2ct\mu_{sd}^2}{\sigma^2 \sqrt{t(\sigma^2 + t\mu_{sd}^2)}} \right) \times \exp \left( -\frac{\sigma^4 (c - \mu_{mean} t)^2 + (c\sigma^2 + t\mu_{mean}\sigma^2 + 2ct\mu_{sd}^2)^2}{t\sigma^4 (\sigma^2 + t\mu_{sd}^2)} \right) \quad (3)$$

where  $\phi(x)$  is the CDF of the standard normal distribution,  $\phi(x) = \frac{1}{\sqrt{2\pi}} \int_{-\infty}^x \exp\left(-\frac{t^2}{2}\right) dt$ . Since  $\mu_{mean}$ ,  $\sigma$ ,  $\mu_{sd}$  can be scaled proportionally to the magnitude of  $c$  keeping  $S(t)$  the same, the value of the initial condition parameter  $c$  has been fixed to be 1.

## iii. Strehler-Mildvan model with vitality drift-diffusion

The Strehler-Mildvan model separates the aging process into two parts. The first part corresponds to the linear loss of vitality, represented by the decaying process of the above stochastic variable  $X(t)$ . The second part mimics age-independent internal or external challenges. If the magnitude of the challenge exceeds the value of the state variable variable  $X(t)$ , the cell is considered dead.

In this exploration, the loss of vitality process is assumed to follow the standard drift-diffusion process, Eq. [2], without introducing drift heterogeneity. The waiting/arrival time  $\tau$  of the age

independent challenge follows exponential distribution with  $p(\tau) = \gamma \exp(-\gamma\tau)$  and  $P(\tau \geq t) = \exp(-\gamma t)$ ,  $t \geq 0$ . The magnitude of a challenge  $m$  also follows an exponential distribution with  $p(m) = \nu \exp(-\nu m)$  and  $P(m \geq M) = \exp(-\nu M)$ .

The survival function  $S_L(t)$  for the drift-diffusion based loss of vitality part of the Strehler-Mildvan model is given (3) by

$$S_L(t) = \phi\left(\frac{c-\mu t}{\sigma\sqrt{t}}\right) - \exp\left(\frac{2c\mu}{\sigma^2}\right) \phi\left(-\frac{c+\mu t}{\sigma\sqrt{t}}\right) \quad (4)$$

On the other hand, the survival function  $S_c(t)$  for the age-independent challenge arrival part of the Strehler-Mildvan model can be derived from the corresponding hazard function  $h(t)$  using

$$S_c(t) = \exp\left(-\int_0^t h(\tau) d\tau\right) \quad (5)$$

The hazard function is given by

$$h(t) = \gamma \int_0^\infty \frac{P(m \geq x | X(t) = x) p(X(t) = x)}{S_L(t)} dx \quad (6)$$

Here, the hazard function is the product of the challenge arrival rate  $\gamma$  and the probability that the challenge kills (represented by the integral). The term inside the integral consists of two parts. The first part  $P(m \geq x | X(t) = x) = \exp(-\nu x)$  denotes the probability that the arrived challenge is greater than the vitality state value  $x$ ; while the second part  $\frac{p(X(t)=x)}{S_L(t)}$  represents the conditional probability that a cell is alive at time  $t$  and its vitality state has a positive value  $x$ . The probability density for a drift-diffusion process, which started at location  $c$  at  $t = 0$  and is at location  $x > 0$  at time  $t$ , is given (3) by

$$p(X(t) = x) = \frac{1}{\sigma\sqrt{2\pi t}} \left\{ \exp\left(-\frac{(x-c+\mu t)^2}{2\sigma^2 t}\right) - \exp\left(-\frac{2c\mu}{\sigma^2}\right) \exp\left(-\frac{(x+c+\mu t)^2}{2\sigma^2 t}\right) \right\} \quad (7)$$

Substituting Eq. [7] and Eq. [4] into Eq. [6], the hazard function for the age-independent challenge arrival part of the Strehler-Mildvan model can then be expressed in terms of cumulative standard normal distribution as follows

$$\begin{aligned} h(t) &= \gamma \int_0^\infty \frac{P(m \geq x | X(t) = x) p(X(t) = x)}{S_L(t)} dx \\ &= \gamma \left[ \exp\left(\frac{1}{2}\nu(-2c + 2\mu t + \mu\sigma^2 t)\right) \right. \\ &\quad \times \left. \left\{ \phi\left(\frac{c - (\mu + \nu\sigma^2)t}{\sigma\sqrt{t}}\right) - \exp\left(\frac{2c(\mu + \nu\sigma^2)}{\sigma^2}\right) \phi\left(-\frac{c + (\mu + \nu\sigma^2)t}{\sigma\sqrt{t}}\right) \right\} \right] \end{aligned}$$

$$/ \left[ \phi \left( \frac{c - \mu t}{\sigma \sqrt{t}} \right) - \exp \left( \frac{2c\mu}{\sigma^2} \right) \phi \left( -\frac{c + \mu t}{\sigma \sqrt{t}} \right) \right] \quad (8)$$

As a result, the overall survival function  $S(t)$  of the Strehler-Mildvan model is given by

$$S(t) = S_L(t) S_c(t) = \left[ \phi \left( \frac{c - \mu t}{\sigma \sqrt{t}} \right) - \exp \left( \frac{2c\mu}{\sigma^2} \right) \phi \left( -\frac{c + \mu t}{\sigma \sqrt{t}} \right) \right] \exp \left( -\int_0^t h(\tau) d\tau \right) = \left[ \phi \left( \frac{c - \mu t}{\sigma \sqrt{t}} \right) - \exp \left( \frac{2c\mu}{\sigma^2} \right) \phi \left( -\frac{c + \mu t}{\sigma \sqrt{t}} \right) \right] \exp \left( -\int_0^t \gamma \left[ \exp \left( \frac{1}{2} v (-2c + 2\mu\tau + \mu\sigma^2\tau) \right) \times \left\{ \phi \left( \frac{c - (\mu + v\sigma^2)\tau}{\sigma \sqrt{\tau}} \right) - \exp \left( \frac{2c(\mu + v\sigma^2)}{\sigma^2} \right) \phi \left( -\frac{c + (\mu + v\sigma^2)\tau}{\sigma \sqrt{\tau}} \right) \right\} \right] d\tau \right) \quad (9)$$

Since  $\mu$ ,  $\sigma$ ,  $v^{-1}$  can be scaled proportionally to the magnitude of  $c$  (keeping  $S(t)$  to be the same), the value of the initial condition parameter  $c$  has been fixed to be 1.

#### Exponentially-distributed challenge arrival process:

To investigate whether the second module (internal/external challenges) of the Strehler-Mildvan model could be the sole driver of the aging process, we decoupled the Strehler-Mildvan model with drift-diffusion into two modules: (1) the linear loss of vitality and (2) age-independent internal or external challenges. The linear loss of vitality by itself has been separately studied in section ii above. In this section, we focus on the second module.

Here, the death event is considered to be only caused by internal/external challenges, with the assumption that there is no linear loss of vitality. Therefore, the vitality state variable  $X(t)$  is fixed at state 1 all the time until death occurs (as in the sample trajectory of a cell in the inset of fig. S15). Similar to the formulations given in section iii above, the waiting/arrival time  $\tau$  of the age independent challenge follows an exponential distribution with  $p(\tau) = \gamma \exp(-\gamma\tau)$  and  $P(\tau \geq t) = \exp(-\gamma t)$ ,  $t \geq 0$ . The magnitude of a challenge  $m$  also follows an exponential distribution with  $p(m) = v \exp(-vm)$  and  $P(m \geq M) = \exp(-vM)$ . With  $X(t) = 1$ , the hazard function and its corresponding survival function  $S(t)$  take the following forms

$$h(t) = \gamma P(m \geq X(t)) = \gamma \exp(-vX(t)) = \gamma \exp(-v) \quad (10)$$

$$S(t) = \exp \left( -\int_0^t h(\tau) d\tau \right) = \exp \left( -\int_0^t \gamma \exp(-v) d\tau \right) = \exp(-\gamma \exp(-v) t) \quad (11)$$

#### **Performance comparisons among the different stochastic models**

To investigate which of the above microscopic processes can lead to the survival dynamics measured from the wild type yeast cells, separately for each process we randomly sampled parameters from wide ranges (table S9), fed these parameters into the survival function

describing each process, and compared the simulated survival curves to the one obtained experimentally from the analysis of 1000 mother cells of the wild-type background.

Semi-infinite random walk	Lower bound	Upper bound	Scale of range	Initial parameter values for fitting	Fitted parameter values
$l$	5	30	linear	10	10
$\beta^-$	0.05	2	linear	0.4306	0.4288
$\beta^+$	0.01	$\beta^- - 0.01$	linear	0.0346	0.0319
<b>Drift-diffusion with drift heterogeneity</b>					
$\mu_{\text{mean}}$	0.005	0.1	linear	0.0418	0.0418
$\sigma$	0.05	0.15	linear	0.0705	0.0707
$\mu_{\text{sd}}$	0.00001	0.01	log	0.0001	0.0001
<b>Strehler-Mildvan with vitality drift-diffusion</b>					
$\mu$	0.001	0.06	log	0.0313	0.0291
$\sigma$	0.01	0.2	linear	0.0464	0.0422
$\gamma$	0.05	10	log	0.1950	0.2942
$\nu$	1	20	linear	4.7391	5.0132
<b>Exponential challenge arrival</b>					
$\gamma$	0.01	10	log	0.0525	0.0526
$\nu$	0.1	20	log	0.3658	0.3677

**table S9. For each microscopic process, parameter ranges used during the sampling process and the fitted parameter values.** Parameter values corresponding to the smallest SSE (against the wild-type survival data) were used as the initial values for the fitting performed by calling MATLAB's *fminsearch* function.

The difference between the simulation results and the experimental data was quantified by calculating the sum of squared errors (SSE). For each microscopic process, we explored a wide range of parameter space (table S9), randomly sampled 200000 parameter sets, generated the corresponding survival curves using the analytical equations described in section IV (i-iii) above, and quantified the differences with the experimental survival curve. The parameter values corresponding to the least SSE after the sampling process (table S9, fig. S14) were then used as the initial values to input into MATLAB's *fminsearch* function for the final fitting.

Using the best-fitting parameter values, survival curves for the different microscopic processes were plotted against the experimentally-obtained survival data (Fig. 4 of main text; fig. S15 of this section). The Strehler-Mildvan model with vitality drift-diffusion displayed the highest degree

of similarity (the smallest SSE of 0.0032) to the experimental survival curve. Neither the deterministic vitality decay modeled by drift-diffusion process (Fig. 4B) nor the exponential challenge arrival process alone (fig. S15) could describe the yeast aging process well.

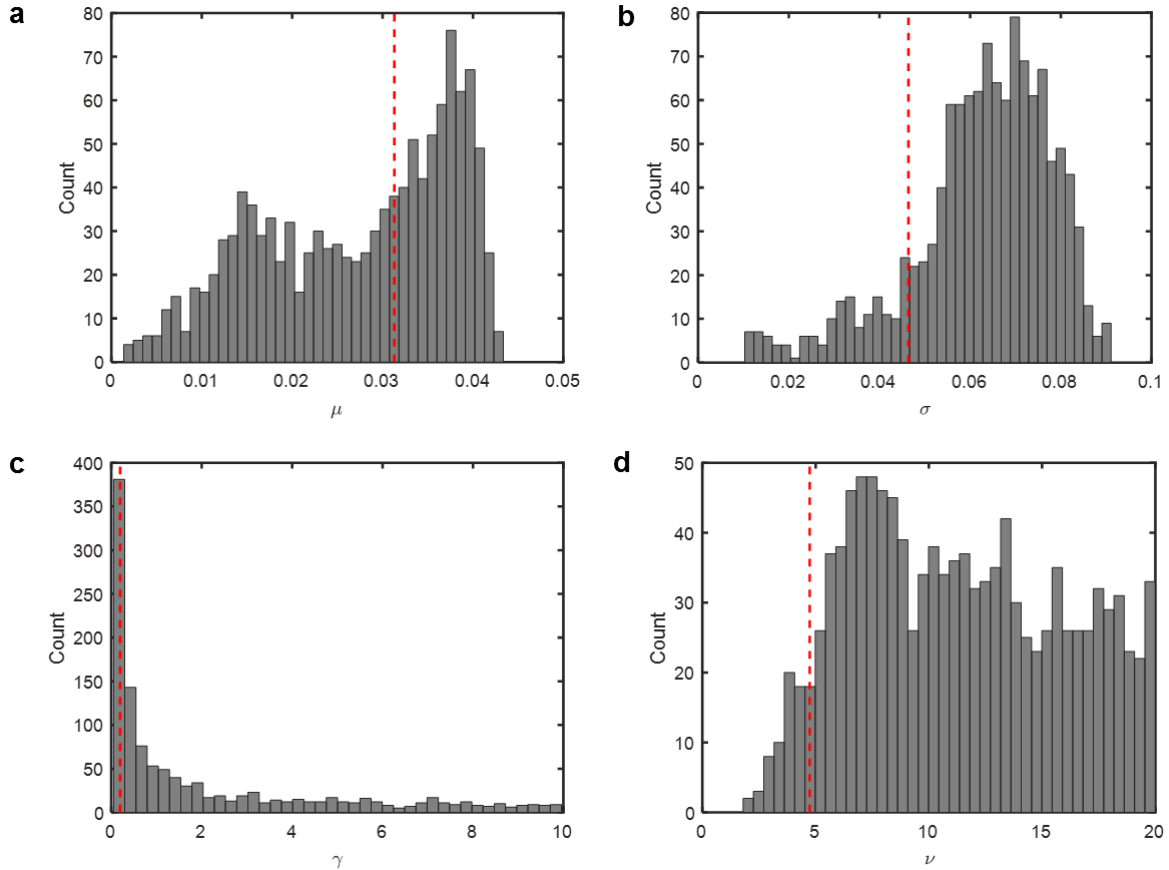


**fig. S14. Simulation results for the Strehler-Mildvan model with vitality drift diffusion. a-d.** By randomly sampling  $N=200000$  parameter sets from the ranges described in table S9, survival distributions were simulated and then the SSE values were calculated against the experimental wild type survival data obtained from tracking 1000 yeast cells. Distributions of  $\mu$ ,  $\sigma$ ,  $\gamma$ ,  $\nu$  corresponding to low deviations ( $0 < \text{SSE} < 0.1$ ) from the wild type survival data are shown here, leading to  $N=1186$  parameter values plotted in each histogram above. Red dashed lines indicate the parameter values corresponding to the smallest SSE.

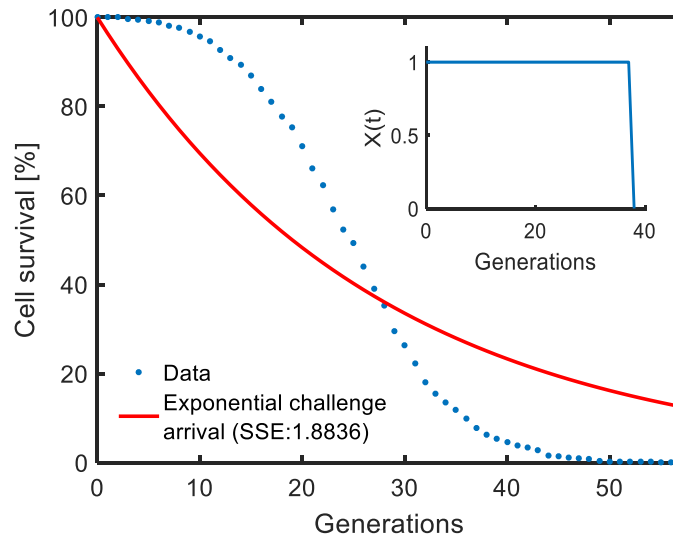
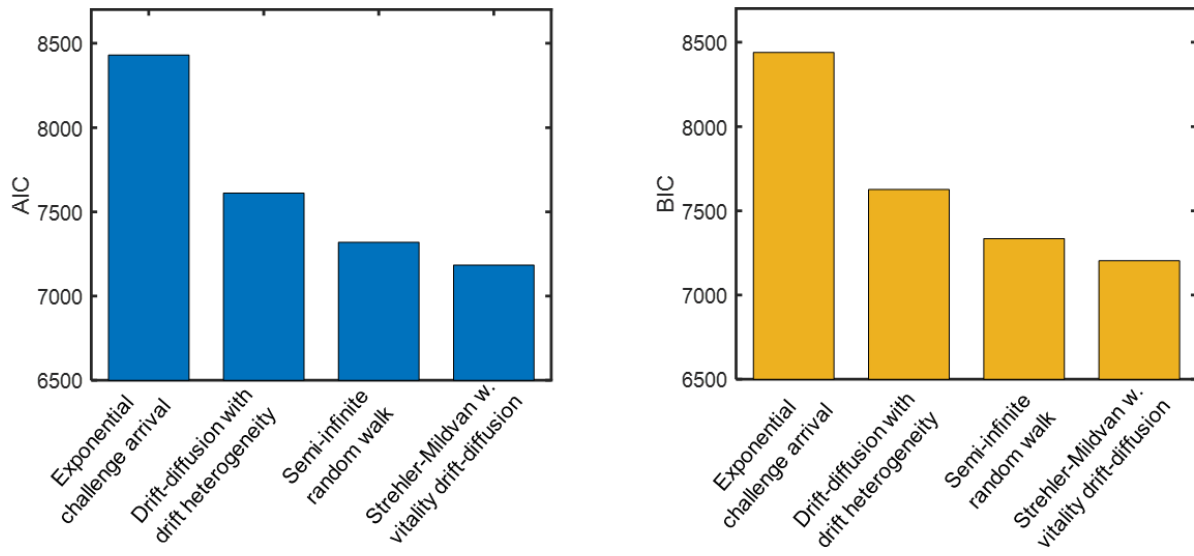


**fig. S15. Performance of the exponential challenge arrival process.**  $N = 200000$  parameter sets were sampled from the parameter ranges described in table S9 and fed into the analytical survival function (Eq. [7]). For each parameter set, the SSE between the simulated survival curve and the experimental survival curve (obtained from the tracking of 1000 wild type cells) was computed. The parameter sets corresponding to the smallest SSE values were then used as initial values for the final optimization process using MATLAB's *fminsearch* function. The red curve was generated by using the optimized/fitted parameter values in the analytical survival function. The experimental survival curve is denoted by the blue dots. The inset shows a schematic trajectory reflecting the nature of the microscopic process.

Since the different stochastic models we tested had different number of parameters, we further applied quantitative tests on the models to see if the Strehler-Mildvan model was indeed the best-performing model. For this goal, we applied the Akaike information criterion (AIC) and Bayesian information criterion (BIC) to the survival data obtained from 1000 wild-type cells. AIC and BIC are similar criteria for model selection among a finite set of models. The model with the lowest AIC or BIC value is preferred. AIC/BIC offers a relative estimate of information lost when a given model is used to represent the process that generates the data. It deals with the trade-off between the goodness of fit of the model and the complexity of the model.

For each stochastic model we tested, the “fitted parameter values” shown in table S9 were used to compute the corresponding log-likelihood values for each model first. These log-likelihood values together with the corresponding number of parameters involved (ranging from 2 to 4 for the different stochastic models) and the number of observations (1000 for each model due to using survival data from 1000 wild-type cells for the fitting process) were then entered into MATLAB's *aicbic* function to compute the corresponding AIC and BIC values for each stochastic model. As shown in figure S16 below, the Strehler-Mildvan model produced the lowest AIC and BIC values, confirming its best-performing status among the different stochastic models tested even when parameter number differences were taken into account.



Model	AIC	BIC
Exponential challenge arrival	8430.2	8440.0
Drift-diffusion with drift heterogeneity	7611.5	7626.2
Semi-infinite random walk	7319.7	7334.4
Strehler-Mildvan w. vitality drift-diffusion	7184.1	7203.7

**fig. S16. Results from the application of AIC and BIC tests on the stochastic models tested.** The Strehler-Mildvan model produced the lowest AIC and BIC values, confirming its best-performing status among the different stochastic models we tested.

We next studied the effect of the parameters used in the Strehler-Mildvan model in addressing the survival dynamics differences between short- and long-living yeast strains. For this characterization, we picked the *sir2Δ* and *fab1Δ* strains. To predict the Strehler-Mildvan parameters for *sir2Δ* and *fab1Δ*, we applied scaling ( $\mu$ ,  $\sigma^2$ ,  $\gamma$ , each multiplied by  $\lambda^{-1}$ ) to the best-fitting parameter values obtained from the wild-type strain. The scaling factor  $\lambda$  for *sir2Δ* and *fab1Δ* was found to be 0.5883 and 1.316 respectively after applying the AFT model to the experimental survival curves of each of these strains together with the wild-type curve. The specific values of the predicted Strehler-Mildvan parameters after applying scaling for *sir2Δ* and *fab1Δ* are provided in table S10. The corresponding survival curves obtained by inputting the predicted parameter values in the Strehler-Mildvan function are shown in fig. S17a. We saw a high degree of similarity between the predicted survival curves and the experimental curves measured from *sir2Δ* and *fab1Δ*, validating the scaled values of the Strehler-Mildvan parameters across these strains (table S10). The relatively higher values of the  $\mu$ ,  $\sigma$ ,  $\gamma$  parameters in the *sir2Δ* background indicate that, compared to the wild-type background, there is higher levels of drift and diffusion in the *sir2Δ* background, together with increased frequency for the age-independent random challenge. The opposite holds for the *fab1Δ* background.



To see if scaling all three of these parameters were needed for predicting the cell survival distributions for *sir2* $\Delta$  and *fob1* $\Delta$ , we scaled only two of the three parameters while keeping the third one to be identical to the value corresponding to the fitted wild-type (fig. S17b-d). We saw that scaling only two of the three parameters ( $\mu$  and  $\gamma$ ) was sufficient for a reasonably good match to the experimental survival curves. The diffusion parameter  $\sigma$ , despite having a similar magnitude as the drift parameter  $\mu$ , does not play an important role in contributing to the differential nature of the aging process among these strains. This suggests that the noise associated with the gradual vitality decay process does not play an important role in affecting the replicative lifespan distribution of yeast cells. In this analysis, the value of  $\nu$  was fixed at the fitted value of 5.0132 (table S10), as generational scaling does not apply to this parameter.

<b>Strehler-Mildvan with vitality drift-diffusion</b>	<i>w.t.</i> (fitted)	<i>sir2</i> $\Delta$ (predicted)	<i>fob1</i> $\Delta$ (predicted)
$\mu$	0.0291	0.0495	0.0221
$\sigma$	0.0422	0.0550	0.0368
$\gamma$	0.2942	0.5001	0.2236
$\nu$	5.0132	5.0132	5.0132

**table S10. Predicted parameter values for *sir2* $\Delta$  and *fob1* $\Delta$  strains, obtained after applying scaling.**

Generational scaling ( $\mu$ ,  $\sigma^2$ ,  $\gamma$ , each multiplied by  $\lambda^{-1}$ ) was applied to the fitted parameter values of the wild-type strain (N=1000 cells) to obtain the corresponding parameter sets for *sir2* $\Delta$  and *fob1* $\Delta$ . The scaling factor  $\lambda$  for *sir2* $\Delta$  and *fob1* $\Delta$  were 0.5883 and 1.316 respectively, obtained after applying the AFT model.

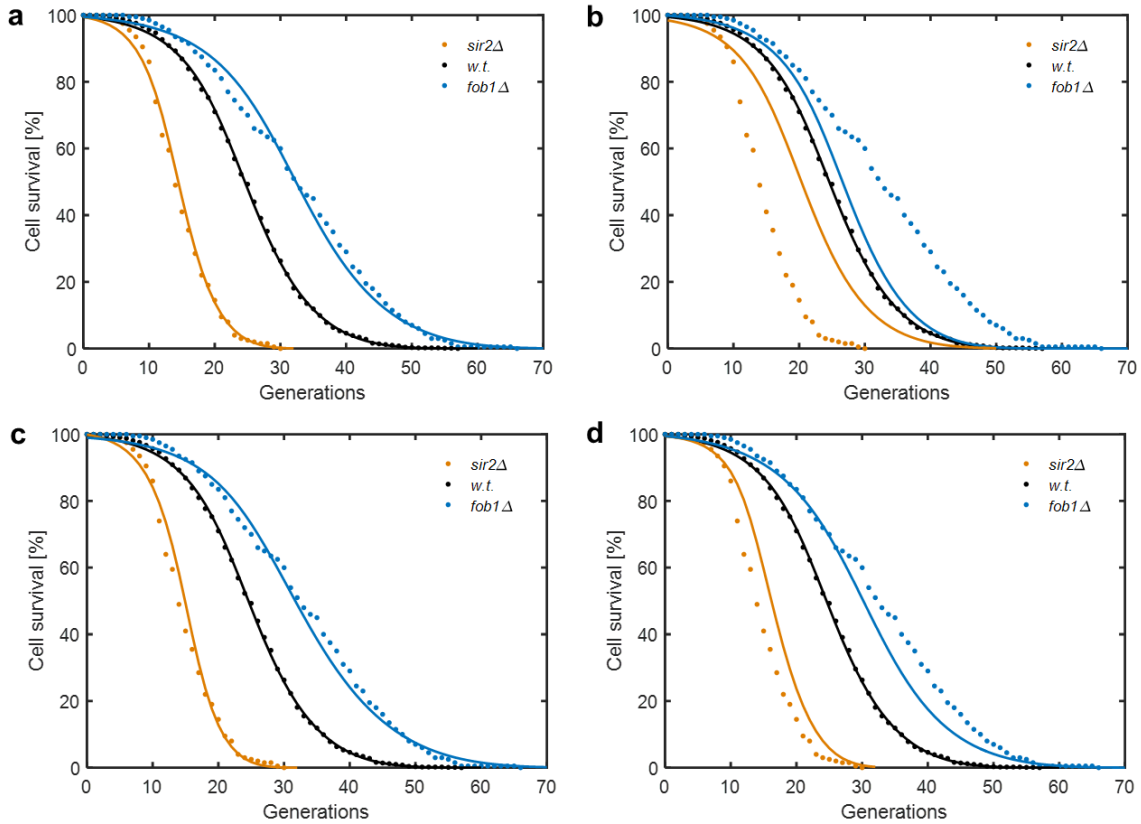


**fig. S17. Sensitivity characterization for the Strehler-Mildvan model parameters.** The solid dots represent the experimental cell survival data obtained from the wild-type (black,  $N=1000$ ), *sir2* $\Delta$  (orange,  $N=200$ ), and *fob1* $\Delta$  (blue,  $N=200$ ) strains. The black solid curve is the survival curve generated using the fitted parameter values for the wild-type strain (table S10). **a.** Based on the fitted parameter values for the wild-type strain (table S10), generational scaling was applied to compute the predicted parameter values for the *sir2* $\Delta$  and *fob1* $\Delta$  strains (table S10). The predicted survival curves for *sir2* $\Delta$  and *fob1* $\Delta$  are shown in solid orange and solid blue, respectively. **b.**  $\mu$  was fixed at the same value as the wild-type strain while generational scaling was applied to predict  $\sigma$  and  $\gamma$ . The predicted survival curves for *sir2* $\Delta$  and *fob1* $\Delta$  are shown in solid orange and solid blue, respectively. **c.**  $\sigma$  was fixed at the same value as the wild-type strain while generational scaling was applied to predict  $\mu$  and  $\gamma$ . The predicted survival curves for *sir2* $\Delta$  and *fob1* $\Delta$  are shown in solid orange and solid blue, respectively. **d.**  $\gamma$  was fixed at the same value as the wild-type strain while generational scaling was applied to predict  $\mu$  and  $\sigma$ . The predicted survival curves for *sir2* $\Delta$  and *fob1* $\Delta$  are shown in solid orange and solid blue, respectively. In all panels, the value of  $v$  was fixed at the fitted value of 5.0132 as generational scaling does not apply to this parameter.

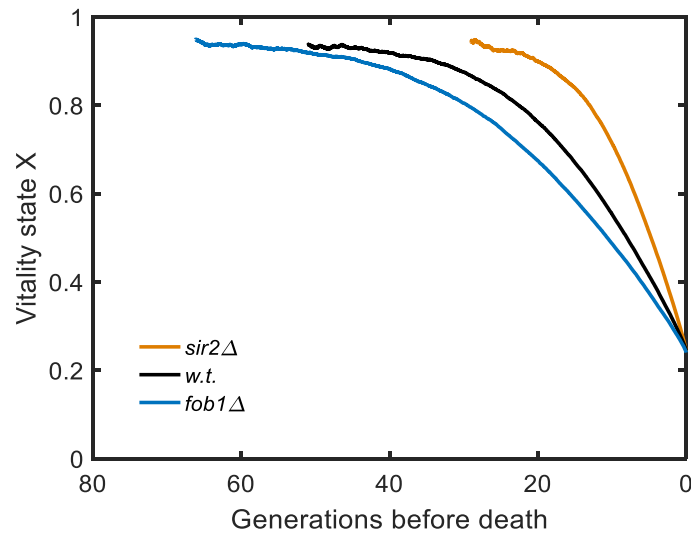


**fig. S18. The generation-dependent dynamics of the aging or viability state X.** Using the strain-specific parameter values displayed in table S10, 10000 stochastic simulations of the Strehler-Mildvan model were ran for each strain. The single cell simulation results for  $X$  were aligned based on the death event at generation 0 and then averaged at each time point prior to death. The small deviations from smoothness at the left of each line is an indication of relatively low cell numbers (due to lifespan variations in each population) included in the averaging process. The threshold cell number used was 100 (at least 100 cells were included for each averaging).

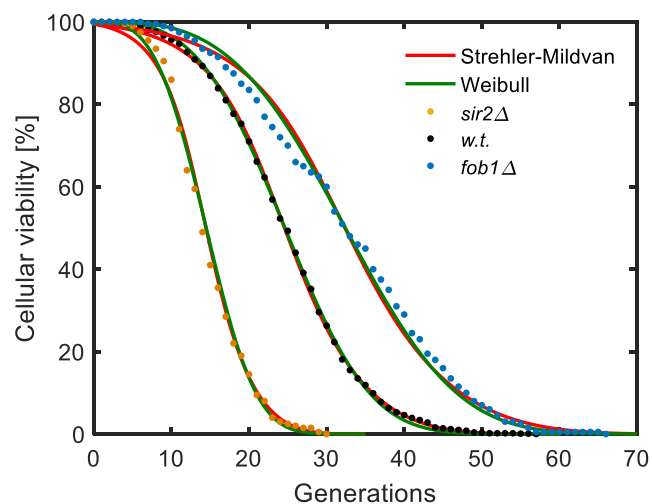


**fig. S19. Numerical connection between the Strehler-Mildvan and Weibull survival functions.** Colored dots show the data while the solid lines indicate the fit (green and red lines on black dots) or simulation results (green and red lines on orange and blue dots). As described above, for temporal scaling to occur for the Strehler-Mildvan function, the parameters  $\mu$ ,  $\sigma^2$ , and  $\gamma$  need to be multiplied by  $\lambda^{-1}$ . On the other hand, for temporal scaling to occur for the Weibull survival function, the parameter  $r$  needs

to be multiplied by  $\lambda^{-1}$ . These suggest the existence of a link between the two functions in terms of  $\mu$ ,  $\sigma^2$ ,  $\gamma$ 's collectively playing the same role as the parameter  $r$ . This figure provides a numerical demonstration of that link. Starting from the parameter values fitted to the data obtained from 1000 WT cells,  $\mu$ ,  $\sigma^2$ ,  $\gamma$  of the Strehler-Mildvan function and  $r$  of the Weibull survival function were rescaled using the same  $\lambda$  corresponding to either the *sir2Δ* (0.5883) or the *fob1Δ* strain (1.316). The resulting curves from the two functions matched well with each other for both cases. The parameter values used in this analysis for the Strehler-Mildvan function are listed in table S10. For the Weibull survival function, the value of parameter  $\alpha$  is fixed at 3.28, while the value (0.0363) of the parameter  $r$  representing the WT cells was obtained from fitting the one-parameter Weibull survival function to the data obtained from the 1000 WT cells' survival curve (black dots). Then, we rescaled the value (0.0363) of the parameter  $r$  using the  $\lambda$  values (0.5883 and 1.316) corresponding to *sir2Δ* and *fob1Δ* strains, respectively. The scaled parameter values were entered into the Weibull survival function to obtain the green lines on the orange and blue dots shown in this figure.